GOVERNING EQUATION DISCOVERY FROM DATA BASED ON DIFFERENTIAL INVARIANTS

Anonymous authors
Paper under double-blind review

ABSTRACT

The explicit governing equation is one of the simplest and most intuitive forms for characterizing physical laws. However, directly discovering partial differential equations (PDEs) from data poses significant challenges, primarily in determining relevant terms from a vast search space. Symmetry, as a crucial prior knowledge in scientific fields, has been widely applied in tasks such as designing equivariant networks and guiding neural PDE solvers. In this paper, we propose a pipeline for governing equation discovery based on differential invariants, which can losslessly reduce the search space of existing equation discovery methods while strictly adhering to symmetry. Specifically, we compute the set of differential invariants corresponding to the infinitesimal generators of the symmetry group and select them as the relevant terms for equation discovery. Taking DI-SINDy (SINDy based on Differential Invariants) as an example, we demonstrate that its success rate and accuracy in PDE discovery surpass those of other symmetry-informed governing equation discovery methods across a series of PDEs. Additional results further indicate that our method exhibits strong robustness to dataset and symmetry noise, significant potential for collaborating with symmetry discovery approaches to solve high-dimensional systems with unknown symmetries, and the ability to serve as a universal plug-and-play module compatible with diverse equation discovery methods.

1 INTRODUCTION

Explicit equations, particularly partial differential equations (PDEs), play a significant role in scientific fields due to their concise and intuitive mathematical forms. Discovering governing equations directly from observational data has become an important topic, and its solutions may serve as AI assistants to human scientists in uncovering new physical laws. Although neural PDE solvers also aim for data-driven evolution prediction (Greydanus et al., 2019; Bar-Sinai et al., 2019; Sanchez-Gonzalez et al., 2020; Li et al., 2020; Thuerey et al., 2021; Brandstetter et al., 2022b; Gupta & Brandstetter, 2022; Takamoto et al., 2022; 2023; Lippe et al., 2023; Kapoor et al., 2023; Cho et al., 2024; Musekamp et al., 2024), their implicit learning approach, compared to explicit equation discovery, suffers from limitations such as lack of interpretability and weaker out-of-distribution (OOD) generalization. In this paper, we formalize the problem as discovering the governing PDE $F(x, u^{(n)}) = 0$ from trajectory data $u(x)$, where $x \in \mathbb{R}^p$ represents the independent variables, $u \in \mathbb{R}^q$ denotes the dependent variables, and $u^{(n)}$ signifies derivatives of u with respect to x up to order n.

Some previous works have made progress on the data-driven equation discovery problem. One category of search-based methods (Schmidt & Lipson, 2009; Gaucel et al., 2014; Petersen et al., 2019; Cranmer et al., 2019; 2020; Udrescu & Tegmark, 2020; La Cava et al., 2021; Mundhenk et al., 2021; Sun et al., 2022; Cranmer, 2023) explores the structure of equations interpretably, but their enormous search space incurs high computational costs. Another category of deep learning-based approaches (Brunton et al., 2016; Champion et al., 2019; Biggio et al., 2021; Messenger & Bortz, 2021; Kamienny et al., 2022) is generally more efficient and versatile, yet still requires pre-specifying key relevant terms of the equation skeleton. To address the limitations of these works, we need to leverage prior knowledge of scientific problems to constrain the form of equations—in other words, to narrow the search space of equations.

Reviewers: please read the Reviewer Guidelines (iclr.cc/Conferences/2027/ReviewerGuidelines) and the AI Policy for Reviewers (iclr.cc/Conferences/2027/AIPolicyForReviewers). If you used AI to expand, edit, or polish your review, please provide the input text to the LLM. Better still, consider skipping the LLM and submitting your original text: we, and the authors, are much more interested in your unedited thoughts than in what an LLM has to say. AI-assisted or not, you are putting your name and reputation behind your review: LLM-generated falsehoods, hallucinations or misrepresentations are subject to disciplinary action, which may include desk-rejecting all papers you have authored.

Symmetry is important prior knowledge in scientific problems, with each symmetry corresponding to a conserved quantity. Recently, some studies have attempted to discover symmetries from data for symmetry-dependent downstream tasks (Benton et al., 2020; Dehmamy et al., 2021; Moskalev et al., 2022; Desai et al., 2022; Yang et al., 2023; 2024a; Ko et al., 2024; Shaw et al., 2024; Hu et al., 2025a). Our goal is to leverage known symmetries to guide the discovery of governing equations. Although Yang et al. (2024b) achieve this by adding explicit symmetry constraints or implicit symmetry regularization terms, the governing equations they identify cannot strictly adhere to general symmetries, and the manually specified equation skeletons significantly affect accuracy.

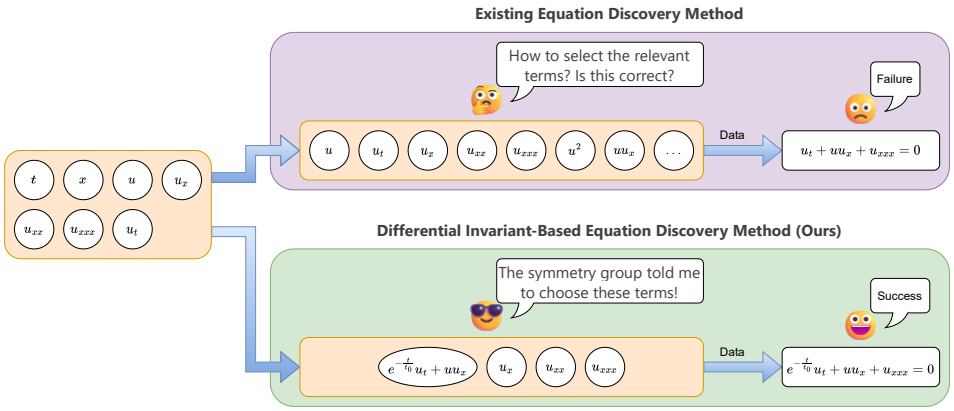

Figure 1: Comparison between the existing equation discovery method and our differential invariant-based equation discovery method for the nKdV equation $e^{-\frac{t}{t_0}}u_t + uu_x + u_{xxx} = 0$. The former struggles with selecting relevant terms, whereas our relevant terms are directly determined by the symmetry group.

In this paper, we implement symmetry-guided equation discovery based on differential invariants. Given the infinitesimal generators of a symmetry group, we can derive their prolongation forms and differential invariants. Then, we directly select these differential invariants as the relevant terms and plug them into any existing equation discovery method, such as SINDy (Brunton et al., 2016). The proposition cited in Section 4.2 will demonstrate that this approach hard-embeds symmetry into the equation skeleton without sacrificing its expressive power. In other words, we "losslessly" compress the search space of equations. As shown in Figure 1, for the relatively complex nKdV equation $e^{-\frac{t}{t_0}}u_t + uu_x + u_{xxx} = 0$, existing equation discovery methods struggle to identify the key relevant terms and construct the correct equation skeleton from a large search space of partial derivatives, whereas our method can accurately determine it by leveraging the information of the symmetry group.

In summary, our contributions are as follows: (1) We propose a method for equation discovery based on differential invariants, which is guided by symmetry groups in the selection of key relevant terms. (2) Using the existing proposition, we substantiate that our method ensures the equation skeleton strictly adheres to symmetry without compromising its expressive power. (3) Taking SINDy based on Differential Invariants (DI-SINDy) as an example, we demonstrate that our method can be plug-and-play with existing equation discovery approaches. (4) The experimental results on a series of PDEs show that our DI-SINDy achieves higher success rates and accuracy compared with baseline methods, while also exhibiting greater stability in long-term predictions. (5) Additional experimental results demonstrate the robustness of our framework against dataset and symmetry noise, its capability to collaborate with symmetry discovery approaches in handling high-dimensional cases with unknown symmetries, and its universality as a plug-and-play module compatible with diverse governing equation discovery methods.

2 Related Work

Symmetry discovery. The application of symmetry in downstream tasks is based on the premise that we know it in advance; otherwise, we first need to discover the symmetry from the data. Some

works discover symmetry based on Lie group and Lie algebra representations (Dehmamy et al., 2021; Moskalev et al., 2022; Desai et al., 2022; Yang et al., 2023; Hu et al., 2025b), but they are limited to linear symmetries. Subsequent works attempt to find more complex nonlinear symmetries (Yang et al., 2024a; Ko et al., 2024; Shaw et al., 2024; Hu et al., 2025a). They utilize the discovered symmetries to guide downstream tasks, achieving performance improvements, which validates the effectiveness of the results. The techniques in this paper can be combined with these symmetry discovery methods to address scenarios where symmetries are not known in advance.

Governing equation discovery. Automatically discovering governing equations from data is an important topic at the intersection of AI and science. One branch of methods relies on search algorithms and has achieved interpretable results. Deep Symbolic Regression (DSR) (Petersen et al., 2019) employs a novel risk-seeking policy gradient to train a recurrent neural network, which emits a distribution over tractable mathematical expressions. Mundhenk et al. (2021) utilize neural-guided search to generate starting populations for a random restart genetic programming component, aiming to solve symbolic regression and other symbolic optimization problems. Symbolic Physics Learner (SPL) (Sun et al., 2022) machine leverages a Monte Carlo Tree Search (MCTS) agent to construct optimal expression trees, which interpret mathematical operations and variables. PySR (Cranmer, 2023) adopts a multi-population evolutionary algorithm and a unique evolve-simplify-optimize loop to accelerate the discovery of symbolic models. However, a limitation of such methods is their low computational efficiency when the search space is large.

Another branch of methods leverages deep learning to improve the efficiency of equation discovery. SINDy (Brunton et al., 2016) employs sparse regression to identify equation forms that are both accurate and concise. Building upon SINDy, Champion et al. (2019) further utilize a deep autoencoder network to transform coordinates into a reduced space where the dynamics can be sparsely represented. Weak SINDy (Messenger & Bortz, 2021) replaces pointwise derivative approximations with linear transformations and variance reduction techniques to enhance the robustness of SINDy against noise. NeSymReS (Biggio et al., 2021) pre-trains a Transformer to predict from an unbounded set of equations. These methods still require assumptions about key relevant terms of the equation skeleton and fail to incorporate scientific prior knowledge to narrow the search space for equations.

Applications of symmetry. Symmetry plays an important role in both traditional mathematical physics problems and the field of deep learning. We summarize related works in Appendix A.

3 Preliminary

Readers unfamiliar with the theory of Lie groups and Lie algebras are strongly encouraged to read Appendix B for formal definitions and Appendix C for concrete illustrative examples.

4 Method

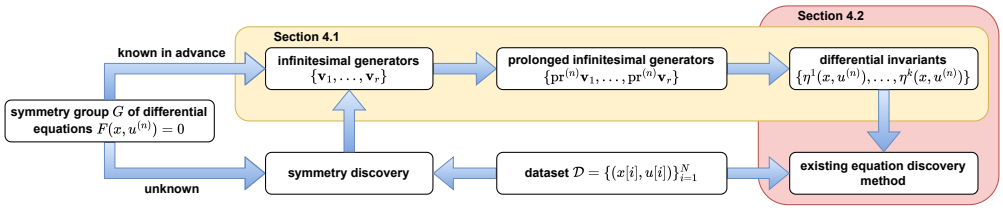

Figure 2: Pipeline of our differential invariant-based equation discovery method.

In short, we explore the use of prior knowledge about the symmetry group G to guide the discovery of governing PDEs $F(x, u^{(n)}) = 0$ from the dataset $\mathcal{D} = \{(x[i], u[i])\}_{i=1}^N$. In Section 4.1, we prolong the infinitesimal generators of the symmetry group and compute the corresponding differential invariants. In Section 4.2, we discuss integrating differential invariants with existing equation discovery methods and provide a proposition to demonstrate that our approach is both correct and complete. In Section 4.3, we take SINDy (Brunton et al., 2016) as an example to showcase the

theoretical advantages of our method over other symmetry-guided equation discovery approaches, such as EquivSINDy-c and EquivSINDy-r (Yang et al., 2024b). Figure 2 provides an intuitive summary of our differential invariant-based equation discovery pipeline. **For readers unfamiliar with the theory of Lie groups and Lie algebras, we strongly recommend referring to the concrete examples in Appendix D to intuitively understand the derivation process of differential invariants.**

4.1 Calculation of Differential Invariants

Differential invariants refer to quantities that remain unchanged under the action of a prolonged group. Definition 2.51 in the textbook (Olver, 1993) provides a formal definition of differential invariants, which we briefly restate as follows.

Definition 4.1 *Let G be a Lie group acting on $X \times U$. An n-th order differential invariant of G is a smooth function $\eta : X \times U^{(n)} \to \mathbb{R}$ such that η is an invariant under the prolonged group action $\mathrm{pr}^{(n)}G$:*

$$\forall g \in G, (x, u^{(n)}) \in X \times U^{(n)} : \quad \eta(\mathrm{pr}^{(n)} g \cdot (x, u^{(n)})) = \eta(x, u^{(n)}). \tag{1}$$

We now discuss how to find the differential invariants of a Lie group G. This problem can be formalized as follows: given the infinitesimal generators $\{\mathbf{v}_1, \ldots, \mathbf{v}_r\}$ of the Lie group G, we seek a complete set of functionally independent n-th order differential invariants $\{\eta^1(x, u^{(n)}), \ldots, \eta^k(x, u^{(n)})\}$ for $\mathrm{pr}^{(n)}G$ (functionally independent: they cannot be expressed as combinations of each other).

The first thing we need to do is derive the n-th order prolongation $\{\mathrm{pr}^{(n)}\mathbf{v}_1, \ldots, \mathrm{pr}^{(n)}\mathbf{v}_r\}$ of the infinitesimal generators. Consider an infinitesimal group action on $X \times U = \mathbb{R}^p \times \mathbb{R}^q$ in the form:

$$\mathbf{v} = \sum_{i=1}^{p} \xi^i(x, u) \frac{\partial}{\partial x^i} + \sum_{\alpha=1}^{q} \phi_\alpha(x, u) \frac{\partial}{\partial u^\alpha}. \tag{2}$$

Then, according to Theorem 2.36 in the textbook (Olver, 1993), its n-th order prolongation is:

$$\mathrm{pr}^{(n)}\mathbf{v} = \mathbf{v} + \sum_{\alpha=1}^{q} \sum_{J} \phi_\alpha^J(x, u^{(n)}) \frac{\partial}{\partial u_J^\alpha}, \tag{3}$$

where the coefficients are determined by:

$$\phi_\alpha^J(x, u^{(n)}) = \mathrm{D}_J \left(\phi_\alpha - \sum_{i=1}^{p} \xi^i u_i^\alpha \right) + \sum_{i=1}^{p} \xi^i u_{J,i}^\alpha. \tag{4}$$

Here, $J = (j_1, \ldots, j_k)$ with $j_i = 1, \ldots, p$ and $k = 1, \ldots, n$, $u_i^\alpha = \frac{\partial u^\alpha}{\partial x^i}$, and $u_{J,i}^\alpha = \frac{\partial u_J^\alpha}{\partial x^i} = \frac{\partial^{k+1} u^\alpha}{\partial x^i \partial x^{j_1} \ldots \partial x^{j_k}}$. Note that D_J denotes the total derivative. For a smooth function $P(x, u^{(n)})$, its relationship with partial derivatives is given by $\mathrm{D}_i P = \frac{\partial P}{\partial x^i} + \sum_{\alpha=1}^{q} \sum_J u_{J,i}^\alpha \frac{\partial P}{\partial u_J^\alpha}$. Taking the infinitesimal group action $\mathbf{v} = -u\frac{\partial}{\partial x} + x\frac{\partial}{\partial u}$ of the SO(2) group as an example, its first-order prolongation is $\mathrm{pr}^{(1)}\mathbf{v} = \mathbf{v} + \phi^x(x, u, u_x)\frac{\partial}{\partial u_x}$, where $\phi^x(x, u, u_x) = \mathrm{D}_x(x + uu_x) - uu_{xx} = 1 + u_x^2$.

Next, we derive the n-th order differential invariants based on the prolonged infinitesimal generators. According to the infinitesimal criteria introduced in Section B, Equation (1) is equivalent to:

$$\mathrm{pr}^{(n)}\mathbf{v}\left[\eta(x, u^{(n)})\right] = \sum_{i=1}^{p} \xi^i(x, u) \frac{\partial \eta}{\partial x^i} + \sum_{\alpha=1}^{q} \phi_\alpha(x, u) \frac{\partial \eta}{\partial u^\alpha} + \sum_{\alpha=1}^{q} \sum_{J} \phi_\alpha^J(x, u^{(n)}) \frac{\partial \eta}{\partial u_J^\alpha} = 0. \tag{5}$$

Then, we construct the characteristic equations:

$$\frac{\mathrm{d}x^i}{\xi^i(x, u)} = \frac{\mathrm{d}u^\alpha}{\phi_\alpha(x, u)} = \frac{\mathrm{d}u_J^\alpha}{\phi_\alpha^J(x, u^{(n)})}, \tag{6}$$

for all $i = 1, \ldots, p$, $\alpha = 1, \ldots, q$, and $J = (j_1, \ldots, j_k)$ with $j_i = 1, \ldots, p$ and $k = 1, \ldots, n$. The integration constants of the general solution to the characteristic equations yield the differential invariants:

$$\eta^1(x, u^{(n)}) = c_1, \ldots, \eta^k(x, u^{(n)}) = c_k. \tag{7}$$

In the case of multiple prolonged infinitesimal generators, we solve the corresponding characteristic equations jointly. Taking the $\mathrm{SO}(2)$ group as an example again, the first-order prolongation of its infinitesimal generator is $\mathrm{pr}^{(1)}\mathbf{v} = -u\frac{\partial}{\partial x} + x\frac{\partial}{\partial u} + (1+u_x^2)\frac{\partial}{\partial u_x}$. We construct the characteristic equation as $\frac{\mathrm{d}x}{-u} = \frac{\mathrm{d}u}{x} = \frac{\mathrm{d}u_x}{1+u_x^2}$. The constants obtained by integration are $\eta^1(x,u,u_x) = \sqrt{x^2+u^2}$ and $\eta^2(x,u,u_x) = \frac{xu_x-u}{uu_x+x}$, which constitute the first-order differential invariants of the $\mathrm{SO}(2)$ group.

4.2 Governing Equation Discovery Based on Differential Invariants

Existing equation discovery methods typically follow the paradigm of first specifying the equation skeleton and then optimizing the parameters. When manually specifying the equation skeleton, the challenge lies in selecting the relevant terms. Including too many irrelevant terms leads to excessive computational costs and reduced accuracy, while omitting key terms makes it theoretically impossible for the algorithm to achieve the correct solution. This limitation becomes even more pronounced in partial differential equation discovery, as compared to $X \times U$, $X \times U^{(n)}$ usually constitutes a much larger search space with more candidate terms to choose from.

Our method aims to use symmetry to guide the selection of relevant terms. We hope that this selection approach, while respecting symmetry, can provide a relatively concise search space without losing expressive power. Proposition 2.56 in the textbook (Olver, 1993) provides the inspiration, which we briefly restate as follows.

Proposition 4.2 *Let G be a Lie group acting on $X \times U$, and $\eta^1(x,u^{(n)}),\dots,\eta^k(x,u^{(n)})$ be a complete set of functionally independent n-th order differential invariants. An n-th order differential equation $F(x,u^{(n)}) = 0$ admits G as a symmetry group if and only if there is an equivalent equation*

$$\widetilde{F}(\eta^1(x,u^{(n)}),\dots,\eta^k(x,u^{(n)})) = 0 \tag{8}$$

involving only the differential invariants of G.

Therefore, we first use the procedure in Section 4.1 to compute differential invariants based on the symmetry group, which serve as all the relevant terms. Then, we can choose any existing equation discovery method (Brunton et al., 2016; Champion et al., 2019; Messenger & Bortz, 2021; Biggio et al., 2021) to explicitly solve for $\widetilde{F}$. Our approach does not interfere with the core of these methods, except for providing the selection of relevant terms, which means it is plug-and-play. Proposition 4.2 theoretically guarantees that this substitution approach strictly adheres to the symmetry prior while ensuring that the equation skeleton is not missing potential solutions due to the omission of relevant terms. When the symmetry is unknown, we can first employ symmetry discovery methods (Yang et al., 2024a; Ko et al., 2024; Shaw et al., 2024) to obtain infinitesimal generators from the data and then implement the aforementioned equation discovery process.

Table 1: The complete set of functionally independent differential invariants corresponding to different numbers of provided infinitesimal generators. For detailed calculation steps, refer to Appendix D.1.

Provided infinitesimal generators	Complete set of functionally independent differential invariants
$\emptyset$	$\{t, x, u, u_t, u_x, u_{xx}, u_{xxx}, u_{xxxx}\}$
$\{\partial_x\}$	$\{t, u, u_t, u_x, u_{xx}, u_{xxx}, u_{xxxx}\}$
$\{\partial_x, \partial_t\}$	$\{u, u_t, u_x, u_{xx}, u_{xxx}, u_{xxxx}\}$
$\{\partial_x, \partial_t, t\partial_x + \partial_u\}$	$\{u_t + uu_x, u_x, u_{xx}, u_{xxx}, u_{xxxx}\}$

Note that we do not need to exhaustively provide all infinitesimal generators of the symmetry group. In most cases, we might miss some infinitesimal generators due to reasons such as errors in symmetry detection, but this does not affect the correctness of the equation discovery results. This is because if a Lie group G is the symmetry group of a differential equation, so is any subgroup $\widetilde{G} \subseteq G$. In fact, each additional correct infinitesimal generator we provide reduces the complete set of functionally independent differential invariants, which leads to a smaller and more accurate search space for the governing equation. In Table 1, we use the Lie point symmetries of the KdV, KS, and Burgers equations mentioned by Ko et al. (2024) as examples to demonstrate the complete set of functionally independent differential invariants corresponding to different numbers of infinitesimal generators.

4.3 EXAMPLE ALGORITHM: DI-SINDY

Now our method can be summarized as follows. First, we use symmetry discovery methods to obtain infinitesimal generators from the dataset if the symmetries are not known a priori. Then, we derive the prolonged infinitesimal generators and compute the differential invariants based on them. Finally, we select the relevant terms of the equation skeleton from the differential invariants and employ existing equation discovery methods to obtain the explicit governing equation. Taking SINDy (Brunton et al., 2016) based on Differential Invariants (DI-SINDy) as an example, we outline the overall workflow in Appendix E.

The EquivSINDy-c and EquivSINDy-r methods proposed by Yang et al. (2024b) also attempt to use symmetry to guide SINDy in discovering governing equations of the form $h(x) = W\Theta(x)$. However, for EquivSINDy-c, it cannot handle nonlinear cases, and Proposition 4.2 in the original paper (Yang et al., 2024b) specifies that $\Theta(x)$ can only be chosen as polynomials. Additionally, the constrained parameter space of W reduces the expressive power of the equation skeleton. On the other hand, the necessity and sufficiency of Proposition 4.2 in this paper guarantee that DI-SINDy's skeleton can fully express all equations satisfying the symmetry, and $\Theta(x)$ can be freely selected, thereby addressing the limitations of EquivSINDy-c. Compared to EquivSINDy-r, which incorporates symmetry loss as a regularization term into SINDy's loss function, DI-SINDy ensures that the equation skeleton strictly adheres to symmetry without requiring hyperparameter tuning for regularization coefficients. Overall, DI-SINDy holds significant theoretical advantages over related works, thanks to its intrinsic ability to "losslessly" compress the equation search space based on symmetry.

5 EXPERIMENT

5.1 EXPERIMENTAL SETUP

Table 2: Explicit expressions, infinitesimal generators of symmetry groups, and corresponding differential invariants for the KdV, KS, Burgers, and nKdV equations Ko et al. (2024).

Name	Equation	Infinitesimal generators	Differential invariants
KdV	$u_t + uu_x + u_{xxx} = 0$		
KS	$u_t + u_{xx} + u_{xxxx} + uu_x = 0$	$\{\frac{\partial}{\partial x}, \frac{\partial}{\partial t}, t\frac{\partial}{\partial x} + \frac{\partial}{\partial u}\}$	$\{u_t + uu_x, u_x, u_{xx}, u_{xxx}, u_{xxxx}\}$
Burgers	$u_t + uu_x - \nu u_{xx} = 0$		
nKdV	$e^{-\frac{t}{t_0}}u_t + uu_x + u_{xxx} = 0$	$\{\frac{\partial}{\partial x}, e^{-\frac{t}{t_0}}\frac{\partial}{\partial t}, t_0(e^{\frac{t}{t_0}} - 1)\frac{\partial}{\partial x} + \frac{\partial}{\partial u}\}$	$\{e^{-\frac{t}{t_0}}u_t + uu_x, u_x, u_{xx}, u_{xxx}, u_{xxxx}\}$

We evaluate our method using the Korteweg-de Vries (KdV) equation, the Kuramoto-Shivashinsky (KS) equation, the Burgers equation, and the nKdV equation from Ko et al. (2024). In Table 2, we present their explicit equations, the infinitesimal generators of their symmetry groups, and the corresponding differential invariants (detailed calculation steps are provided in Appendix D), where the prolongation order is specified as fourth-order. We assume the symmetries are known a priori, and the experimental task is to automatically discover the governing equations from the generated data. The infinitesimal generators provided here are all sufficiently simple to be easily obtained by existing symmetry discovery methods. We provide the data generation process in Appendix F.

Taking DI-SINDy presented in Algorithm 1 as an example, we compare it with SINDy (Brunton et al., 2016) and EquivSINDy-r (Yang et al., 2024b). The Lie point symmetry of PDEs is typically nonlinear, which renders EquivSINDy-c inapplicable—hence we exclude it from the comparison. The idea behind EquivSINDy-r is to incorporate the infinitesimal criterion of the symmetry group as a regularization term into the objective function of SINDy, thereby softly constraining the equation skeleton to adhere to the symmetry. The original paper (Yang et al., 2024b) only provides the form of the regularization term for ODE cases. To extend it to PDE scenarios for comparison, we adopt the infinitesimal criterion of Lie point symmetry introduced in Section B as the regularization term:

$$\mathcal{L}_{symm} = \mathbb{E}_{x,u}\left\{\sum_{\mathbf{v}\in V(\mathfrak{g})}\left\|\mathrm{pr}^{(n)}\mathbf{v}\left[F(x,u^{(n)})\right]\right\|^2\right\}, \tag{9}$$

where $V(\mathfrak{g})$ is the set of infinitesimal generators of the symmetry group, and F represents the equation skeleton of SINDy. Then, the overall objective function of EquivSINDy-r is:

$$\mathcal{L}_{total} = \mathcal{L}_{SINDy} + \lambda \cdot \mathcal{L}_{symm}. \tag{10}$$

For a comprehensive comparison, we will traverse the regularization weight hyperparameter $\lambda = \{10^{-3}, 10^{-2}, 10^{-1}\}$.

As described in Algorithm 1, the relevant terms of DI-SINDy are selected as the set of differential invariants shown in Table 2, and the function library Θ is specified as linear terms. For SINDy and EquivSINDy-r, we define the equation skeleton of the KdV, KS, and Burgers equations as $u_t = W\Theta(u, u_x, u_{xx}, u_{xxx}, u_{xxxx})$, and the equation skeleton of the nKdV equation as $e^{-\frac{t}{t_0}} u_t = W\Theta(u, u_x, u_{xx}, u_{xxx}, u_{xxxx})$, where Θ contains terms up to second order. It can be observed that the baseline methods require strong prior assumptions about the equation skeleton during the experimental preparation phase, even though we have manually specified relatively simple forms for them that include the ground truth. More implementation details can be found in Appendix G.

5.2 Quantitative Metrics and Result Analysis

After training with SINDy and its variant methods, we get explicit equations such as $u_t = W\Theta(u, u_x, \dots)$ (for KdV, KS, and Burgers equations) or $e^{-\frac{t}{t_0}} u_t = W\Theta(u, u_x, \dots)$ (for the nKdV equation). In practice, the coefficient matrix is obtained via element-wise multiplication $W = C \odot M$, where C represents the values of each term's coefficient, and the binary mask matrix M indicates whether each term is retained (1 for retained, 0 for discarded). We follow the quantitative metrics introduced by Yang et al. (2024b), which we restate as follows. We consider the discovery of an equation successful if the retained terms in the final result are correct and complete (formally, $M = M^*$, where M^* is the ground truth of the binary mask matrix). We run each experiment 50 times and calculate its **success rate**, which is the most important quantitative metric for explicit equation discovery, as it reflects whether the model can correctly identify the interaction relationships between variables. Furthermore, we use the RMSE of the coefficient matrix, $\sqrt{\frac{1}{n}\sum_{i=1}^{n} \|W - W^*\|^2}$, to evaluate the accuracy of equation discovery, where n is the number of runs, and W^* is the ground truth of the coefficient matrix. We report **RMSE (successful)** and **RMSE (all)**, which represent the RMSE for successful runs and all runs, respectively.

The success rates and RMSE of different SINDy-based methods are presented in Table 3. For the KdV, Burgers, and nKdV equations, EquivSINDy-r, with its soft symmetry constraints, significantly improves both the success rate and accuracy compared to SINDy, while our DI-SINDy further increases the success rate to nearly 100%. Notably, both SINDy and EquivSINDy-r fail for the KS equation, as the KS equation involves a fourth-order derivative term, making finite difference methods prone to large errors in the presence of noise. In contrast, DI-SINDy, benefiting from a smaller search space, can still accurately identify the correct equation form, demonstrating stronger robustness.

Beyond quantitative advantages, as discussed in Section 5.1, DI-SINDy employs differential invariants as candidate terms, unlike SINDy and EquivSINDy-r, which rely on manually specified equation skeletons (e.g., for the nKdV equation, the term $e^{-\frac{t}{t_0}} u_t$ is difficult to guess, whereas differential invariants naturally guide its inclusion). Additionally, the performance of EquivSINDy-r is sensitive to the regularization weight λ, while DI-SINDy eliminates the need for hyperparameter tuning.

We further numerically integrate the discovered explicit equations for the 4 initial conditions in the test dataset and calculate the MSE against their corresponding true trajectories, which we refer to as the **long-term prediction error**. In Figure 3, we visualize the long-term prediction errors of all SINDy-based methods for the KdV, KS, Burgers, and nKdV equations as a function of the integration time steps. We use the ground-truth equation form as the benchmark (blue lines), for which the long-term prediction error primarily stems from finite differences and numerical integration. For the KdV and nKdV equations, the error curves of SINDy and EquivSINDy-r ($\lambda = 10^{-3}$) almost overlap, while for the KS equation, the error curves of SINDy and EquivSINDy-r with all λ values nearly coincide. This is due to the minimal differences in their discovered explicit equations, which can be verified by the numerical results in Table 3. For all PDEs, our DI-SINDy achieves significantly lower long-term prediction errors than baselines, further validating the accuracy of its equation discovery results.

Table 3: Success rates and RMSE of different SINDy-based methods for the KdV, KS, Burgers, and nKdV equations. All experimental results are averaged over 50 runs. RMSE is presented in the format of mean ± std.

Name	Method	Success rate (↑)	RMSE (successful) (↓)	RMSE (all) (↓)
KdV	SINDy	72%	$(2.24 \pm 0.51) \times 10^{-1}$	$(4.42 \pm 3.51) \times 10^{-1}$
	EquivSINDy-r ($\lambda = 10^{-3}$)	72%	$(2.23 \pm 0.51) \times 10^{-1}$	$(4.41 \pm 3.51) \times 10^{-1}$
	EquivSINDy-r ($\lambda = 10^{-2}$)	74%	$(2.18 \pm 0.50) \times 10^{-1}$	$(9.28 \pm 14.01) \times 10^{-2}$
	EquivSINDy-r ($\lambda = 10^{-1}$)	82%	$(1.66 \pm 0.37) \times 10^{-1}$	$(3.16 \pm 3.22) \times 10^{-1}$
	DI-SINDy (Ours)	**100%**	$\mathbf{(2.71 \pm 2.44) \times 10^{-2}}$	$\mathbf{(2.71 \pm 2.44) \times 10^{-2}}$
KS	SINDy	0%	N/A	1.00 ± 0.00
	EquivSINDy-r ($\lambda = 10^{-3}$)	0%	N/A	1.00 ± 0.00
	EquivSINDy-r ($\lambda = 10^{-2}$)	0%	N/A	1.00 ± 0.00
	EquivSINDy-r ($\lambda = 10^{-1}$)	0%	N/A	1.00 ± 0.00
	DI-SINDy (Ours)	**100%**	$\mathbf{(6.18 \pm 0.37) \times 10^{-2}}$	$\mathbf{(6.18 \pm 0.37) \times 10^{-2}}$
Burgers	SINDy	4%	$(2.11 \pm 0.14) \times 10^{-2}$	$(1.52 \pm 2.34) \times 10^{-1}$
	EquivSINDy-r ($\lambda = 10^{-3}$)	16%	$(2.59 \pm 0.42) \times 10^{-2}$	$(1.86 \pm 4.12) \times 10^{-1}$
	EquivSINDy-r ($\lambda = 10^{-2}$)	68%	$(8.06 \pm 3.38) \times 10^{-3}$	$(9.78 \pm 38.08) \times 10^{-2}$
	EquivSINDy-r ($\lambda = 10^{-1}$)	78%	$(9.68 \pm 3.89) \times 10^{-4}$	$(7.03 \pm 35.62) \times 10^{-2}$
	DI-SINDy (Ours)	**98%**	$\mathbf{(2.66 \pm 1.32) \times 10^{-4}}$	$\mathbf{(4.02 \pm 9.62) \times 10^{-4}}$
nKdV	SINDy	20%	$(3.77 \pm 0.14) \times 10^{-1}$	$(8.75 \pm 2.49) \times 10^{-1}$
	EquivSINDy-r ($\lambda = 10^{-3}$)	20%	$(3.76 \pm 0.14) \times 10^{-1}$	$(8.75 \pm 2.50) \times 10^{-1}$
	EquivSINDy-r ($\lambda = 10^{-2}$)	22%	$(3.62 \pm 0.13) \times 10^{-1}$	$(8.60 \pm 2.64) \times 10^{-1}$
	EquivSINDy-r ($\lambda = 10^{-1}$)	44%	$(2.70 \pm 0.19) \times 10^{-1}$	$(6.79 \pm 3.63) \times 10^{-1}$
	DI-SINDy (Ours)	**100%**	$\mathbf{(5.05 \pm 3.84) \times 10^{-2}}$	$\mathbf{(5.05 \pm 3.84) \times 10^{-2}}$

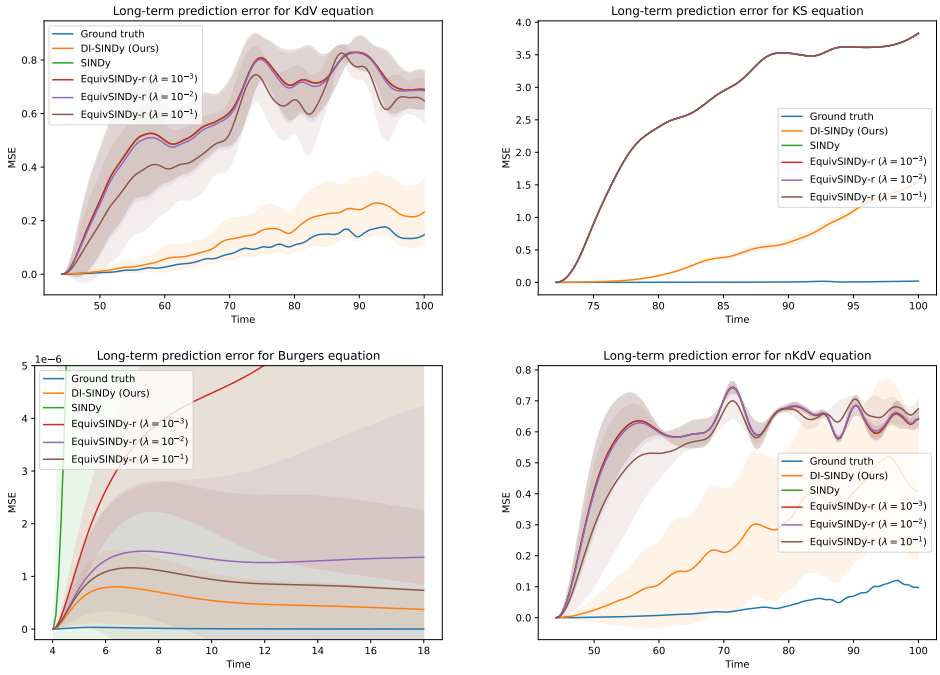

Figure 3: Long-term prediction errors of different SINDy-based methods for the KdV, KS, Burgers, and nKdV equations. The MSE at each time step is averaged over 4 initial conditions and 50 runs, with the shaded area representing the standard deviation.

5.3 Robust Analysis Against Dataset and Infinitesimal Generator Noise

We test the stability of our DI-SINDy method through robustness experiments under conditions such as dataset noise and inaccurate symmetry priors. First, we progressively increase the noise level ($\sigma = \{3 \times 10^{-3}, 5 \times 10^{-3}\}$) on the Burgers equation dataset. The results show that DI-SINDy maintains a high identification success rate and prediction accuracy even when the standard SINDy method fails completely, demonstrating its strong robustness against real-world data interference. Second, we simulate scenarios with deviations in the infinitesimal generator (relative perturbation amplitude $\delta = \{10^{-1}, 3 \times 10^{-1}, 5 \times 10^{-1}\}$) and find that DI-SINDy also exhibits high tolerance, outperforming symmetry-agnostic SINDy when $\delta \leq 3 \times 10^{-1}$, highlighting its potential for integration with symmetry discovery methods. Detailed experimental setups and result analyses are provided in Appendices H.1 and H.2.

5.4 High-Dimensional Case with Unknown Symmetries: Governing Equation Discovery for Reaction-Diffusion System

In the high-dimensional case study of reaction-diffusion systems, we validate the capability of the DI-SINDy method in discovering complex partial differential equations. Given that the symmetries of the system are unknown, we first employ LieNLSD (Hu et al., 2025a) (a method for explicitly discovering nonlinear symmetries) to obtain its infinitesimal generators. Then, by leveraging differential invariant theory, the method compresses the original search space from hundreds of terms to just 9 terms composed of 5 key invariants, constructing a concise equation skeleton. Experimental results demonstrate that DI-SINDy accurately uncovers the governing equations of the system, including the correct structures of nonlinear reaction and diffusion terms, proving its effectiveness in handling high-dimensional dynamical systems. In contrast, traditional SINDy and EquivSINDy-r methods fail due to the curse of dimensionality. We further find that the pipeline can benchmark symmetry discovery methods by comparing results under different symmetry sources. Detailed experimental setups, theoretical derivations, and result analyses are provided in Appendix H.3.

5.5 Differential Invariants as a Plug-and-Play Module for Equation Discovery

Furthermore, we validate the universality of differential invariants by combining them with three additional equation discovery methods: E2E (Kamienny et al., 2022), Weak SINDy (Messenger & Bortz, 2021), and PySR (Cranmer, 2023). Experiments demonstrate that the differential invariant-enhanced variants (DI-E2E, DI-WSINDy, and DI-PySR) consistently outperform their respective baselines across all test equations. Notably, DI-E2E achieves significant performance improvements on the KdV, KS, Burgers, nKdV, and reaction-diffusion equations, with higher prediction accuracy, better stability, and shorter inference time. Particularly in complex high-dimensional reaction-diffusion systems, DI-E2E achieves an almost perfect fit ($R^2 \approx 1$), whereas the original E2E method fails completely. DI-WSINDy and DI-PySR exhibit similar substantial gains, confirming that differential invariants work as a universal plug-and-play module regardless of the downstream regression algorithm. Detailed experimental setups and result analyses are provided in Appendix H.4.

6 Conclusion

Overall, our method addresses several pain points in existing equation discovery approaches. For the large search space of PDEs, most methods struggle to identify the correct relevant terms, whereas we overcome this limitation by employing differential invariants. The necessity and sufficiency of Proposition 4.2 show that our method neither loses expressiveness like symmetry-constrained approaches such as EquivSINDy-c, nor violates symmetry principles like regularization-based methods such as EquivSINDy-r. We hope that our method, in conjunction with established symmetry discovery efforts, will form a systematic solution for complex scientific problems in the future. This vision naturally raises several practical questions (how sensitive is the method to imperfect symmetry priors, how should the prolongation order be chosen, and when is equation discovery from data theoretically well-posed) which we discuss in Appendix I.

AI USE STATEMENT

We used generative AI tools to aid or polish writing. The tools suggested revisions to improve clarity and readability, which the human authors reviewed and decided whether to adopt. The authors take full responsibility for the final content of this paper, including all AI-assisted material.

REFERENCES

Tara Akhound-Sadegh, Laurence Perreault-Levasseur, Johannes Brandstetter, Max Welling, and Siamak Ravanbakhsh. Lie point symmetry and physics-informed networks. *Advances in Neural Information Processing Systems*, 36:42468–42481, 2023.

Shivam Arora, Alex Bihlo, and Francis Valiquette. Invariant physics-informed neural networks for ordinary differential equations. *Journal of Machine Learning Research*, 25(233):1–24, 2024.

Yohai Bar-Sinai, Stephan Hoyer, Jason Hickey, and Michael P Brenner. Learning data-driven discretizations for partial differential equations. *Proceedings of the National Academy of Sciences*, 116(31):15344–15349, 2019.

Gregory Benton, Marc Finzi, Pavel Izmailov, and Andrew G Wilson. Learning invariances in neural networks from training data. *Advances in Neural Information Processing Systems*, 33: 17605–17616, 2020.

Luca Biggio, Tommaso Bendinelli, Alexander Neitz, Aurelien Lucchi, and Giambattista Parascandolo. Neural symbolic regression that scales. In *International Conference on Machine Learning*, pp. 936–945. Pmlr, 2021.

George Bluman and Stephen Anco. *Symmetry and integration methods for differential equations*, volume 154. Springer Science & Business Media, 2008.

George W Bluman. *Applications of symmetry methods to partial differential equations*. Springer, 2010.

Johannes Brandstetter, Max Welling, and Daniel E Worrall. Lie point symmetry data augmentation for neural PDE solvers. In *International Conference on Machine Learning*, pp. 2241–2256. PMLR, 2022a.

Johannes Brandstetter, Daniel Worrall, and Max Welling. Message passing neural PDE solvers. *arXiv preprint arXiv:2202.03376*, 2022b.

Steven L Brunton, Joshua L Proctor, and J Nathan Kutz. Discovering governing equations from data by sparse identification of nonlinear dynamical systems. *Proceedings of the National Academy of Sciences*, 113(15):3932–3937, 2016.

Kathleen Champion, Bethany Lusch, J Nathan Kutz, and Steven L Brunton. Data-driven discovery of coordinates and governing equations. *Proceedings of the National Academy of Sciences*, 116(45): 22445–22451, 2019.

Woojin Cho, Minju Jo, Haksoo Lim, Kookjin Lee, Dongeun Lee, Sanghyun Hong, and Noseong Park. Parameterized physics-informed neural networks for parameterized PDEs. *arXiv preprint arXiv:2408.09446*, 2024.

Miles Cranmer. Interpretable machine learning for science with PySR and SymbolicRegression. jl. *arXiv preprint arXiv:2305.01582*, 2023.

Miles Cranmer, Alvaro Sanchez Gonzalez, Peter Battaglia, Rui Xu, Kyle Cranmer, David Spergel, and Shirley Ho. Discovering symbolic models from deep learning with inductive biases. *Advances in Neural Information Processing Systems*, 33:17429–17442, 2020.

Miles D Cranmer, Rui Xu, Peter Battaglia, and Shirley Ho. Learning symbolic physics with graph networks. *arXiv preprint arXiv:1909.05862*, 2019.

Nima Dehmamy, Robin Walters, Yanchen Liu, Dashun Wang, and Rose Yu. Automatic symmetry discovery with Lie algebra convolutional network. *Advances in Neural Information Processing Systems*, 34:2503–2515, 2021.

Krish Desai, Benjamin Nachman, and Jesse Thaler. Symmetry discovery with deep learning. *Physical Review D*, 105(9):096031, 2022.

Marc Finzi, Max Welling, and Andrew Gordon Wilson. A practical method for constructing equivariant multilayer perceptrons for arbitrary matrix groups. In *International Conference on Machine Learning*, pp. 3318–3328. PMLR, 2021.

Sébastien Gaucel, Maarten Keijzer, Evelyne Lutton, and Alberto Tonda. Learning dynamical systems using standard symbolic regression. In *European Conference on Genetic Programming*, pp. 25–36. Springer, 2014.

Samuel Greydanus, Misko Dzamba, and Jason Yosinski. Hamiltonian neural networks. *Advances in Neural Information Processing Systems*, 32, 2019.

Jayesh K Gupta and Johannes Brandstetter. Towards multi-spatiotemporal-scale generalized PDE modeling. *arXiv preprint arXiv:2209.15616*, 2022.

Lexiang Hu, Yikang Li, and Zhouchen Lin. Explicit discovery of nonlinear symmetries from dynamic data. In *Forty-second International Conference on Machine Learning*, 2025a.

Lexiang Hu, Yikang Li, and Zhouchen Lin. Symmetry discovery for different data types. *Neural Networks*, pp. 107481, 2025b.

Lexiang Hu, Yisen Wang, and Zhouchen Lin. Incorporating arbitrary matrix group equivariance into kans. In *Forty-second International Conference on Machine Learning*, 2025c.

Peter Ellsworth Hydon. *Symmetry methods for differential equations: a beginner's guide*. Number 22. Cambridge University Press, 2000.

N Kh Ibragimov. *Elementary Lie group analysis and ordinary differential equations*, volume 197. Wiley New York, 1999.

Pierre-Alexandre Kamienny, Stéphane d'Ascoli, Guillaume Lample, and François Charton. End-to-end symbolic regression with transformers. *Advances in Neural Information Processing Systems*, 35:10269–10281, 2022.

Taniya Kapoor, Abhishek Chandra, Daniel Tartakovsky, Hongrui Wang, Alfredo Núñez, and Rolf Dollevoet. Neural oscillators for generalizing parametric PDEs. In *The Symbiosis of Deep Learning and Differential Equations III*, 2023.

Gyeonghoon Ko, Hyunsu Kim, and Juho Lee. Learning infinitesimal generators of continuous symmetries from data. *Advances in Neural Information Processing Systems*, 37:85973–86003, 2024.

Risi Kondor and Shubhendu Trivedi. On the generalization of equivariance and convolution in neural networks to the action of compact groups. In *International Conference on Machine Learning*, pp. 2747–2755. PMLR, 2018.

William La Cava, Bogdan Burlacu, Marco Virgolin, Michael Kommenda, Patryk Orzechowski, Fabrício Olivetti de França, Ying Jin, and Jason H Moore. Contemporary symbolic regression methods and their relative performance. *Advances in Neural Information Processing Systems*, 2021 (DB1):1, 2021.

Pierre-Yves Lagrave and Eliot Tron. Equivariant neural networks and differential invariants theory for solving partial differential equations. In *Physical Sciences Forum*, volume 5, pp. 13. MDPI, 2022.

Ye Li, Yiwen Pang, and Bin Shan. Physics-guided data augmentation for learning the solution operator of linear differential equations. In *2022 IEEE 8th International Conference on Cloud Computing and Intelligent Systems (CCIS)*, pp. 543–547. IEEE, 2022.

Yikang Li, Yeqing Qiu, Yuxuan Chen, Lingshen He, and Zhouchen Lin. Affine equivariant networks based on differential invariants. In *Proceedings of the IEEE/CVF conference on computer vision and pattern recognition*, pp. 5546–5556, 2024.

Yikang Li, Yeqing Qiu, Yuxuan Chen, and Zhouchen Lin. Affine steerable equivariant layer for canonicalization of neural networks. In *The Thirteenth International Conference on Learning Representations*, 2025.

Zongyi Li, Nikola Kovachki, Kamyar Azizzadenesheli, Burigede Liu, Kaushik Bhattacharya, Andrew Stuart, and Anima Anandkumar. Fourier neural operator for parametric partial differential equations. *arXiv preprint arXiv:2010.08895*, 2020.

Phillip Lippe, Bas Veeling, Paris Perdikaris, Richard Turner, and Johannes Brandstetter. PDE-Refiner: Achieving accurate long rollouts with neural PDE solvers. *Advances in Neural Information Processing Systems*, 36:67398–67433, 2023.

Robert I McLachlan. On the numerical integration of ordinary differential equations by symmetric composition methods. *SIAM Journal on Scientific Computing*, 16(1):151–168, 1995.

Daniel A Messenger and David M Bortz. Weak SINDy: Galerkin-based data-driven model selection. *Multiscale Modeling & Simulation*, 19(3):1474–1497, 2021.

Artem Moskalev, Anna Sepliarskaia, Ivan Sosnovik, and Arnold Smeulders. LieGG: Studying learned Lie group generators. *Advances in Neural Information Processing Systems*, 35:25212–25223, 2022.

Terrell Mundhenk, Mikel Landajuela, Ruben Glatt, Claudio P Santiago, Brenden K Petersen, et al. Symbolic regression via deep reinforcement learning enhanced genetic programming seeding. *Advances in Neural Information Processing Systems*, 34:24912–24923, 2021.

Daniel Musekamp, Marimuthu Kalimuthu, David Holzmüller, Makoto Takamoto, and Mathias Niepert. Active learning for neural PDE solvers. *arXiv preprint arXiv:2408.01536*, 2024.

Peter J Olver. *Applications of Lie groups to differential equations*, volume 107. Springer Science & Business Media, 1993.

Brenden K Petersen, Mikel Landajuela, T Nathan Mundhenk, Claudio P Santiago, Soo K Kim, and Joanne T Kim. Deep symbolic regression: Recovering mathematical expressions from data via risk-seeking policy gradients. *arXiv preprint arXiv:1912.04871*, 2019.

David Ruhe, Johannes Brandstetter, and Patrick Forré. Clifford group equivariant neural networks. *Advances in Neural Information Processing Systems*, 36:62922–62990, 2023.

Alvaro Sanchez-Gonzalez, Jonathan Godwin, Tobias Pfaff, Rex Ying, Jure Leskovec, and Peter Battaglia. Learning to simulate complex physics with graph networks. In *International Conference on Machine Learning*, pp. 8459–8468. PMLR, 2020.

Vıctor Garcia Satorras, Emiel Hoogeboom, and Max Welling. E(n) equivariant graph neural networks. In *International Conference on Machine Learning*, pp. 9323–9332. PMLR, 2021.

Michael Schmidt and Hod Lipson. Distilling free-form natural laws from experimental data. *science*, 324(5923):81–85, 2009.

Ben Shaw, Abram Magner, and Kevin Moon. Symmetry discovery beyond affine transformations. *Advances in Neural Information Processing Systems*, 37:112889–112918, 2024.

Zakhar Shumaylov, Peter Zaika, James Rowbottom, Ferdia Sherry, Melanie Weber, and Carola-Bibiane Schönlieb. Lie algebra canonicalization: Equivariant neural operators under arbitrary Lie groups. *arXiv preprint arXiv:2410.02698*, 2024.

Zakhar Shumaylov, Peter Zaika, Philipp Scholl, Gitta Kutyniok, Lior Horesh, and Carola-Bibiane Schönlieb. When is a system discoverable from data? discovery requires chaos. *arXiv preprint arXiv:2511.08860*, 2025.

Fangzheng Sun, Yang Liu, Jian-Xun Wang, and Hao Sun. Symbolic physics learner: Discovering governing equations via Monte Carlo tree search. *arXiv preprint arXiv:2205.13134*, 2022.

Makoto Takamoto, Timothy Praditia, Raphael Leiteritz, Daniel MacKinlay, Francesco Alesiani, Dirk Pflüger, and Mathias Niepert. PDEBench: An extensive benchmark for scientific machine learning. *Advances in Neural Information Processing Systems*, 35:1596–1611, 2022.

Makoto Takamoto, Francesco Alesiani, and Mathias Niepert. Learning neural PDE solvers with parameter-guided channel attention. In *International Conference on Machine Learning*, pp. 33448–33467. PMLR, 2023.

Nils Thuerey, Philipp Holl, Maximilian Mueller, Patrick Schnell, Felix Trost, and Kiwon Um. Physics-based deep learning. *arXiv preprint arXiv:2109.05237*, 2021.

Silviu-Marian Udrescu and Max Tegmark. AI Feynman: A physics-inspired method for symbolic regression. *Science advances*, 6(16):eaay2631, 2020.

Amy Xiang Wang, Zakhar Shumaylov, Peter Zaika, Ferdia Sherry, and Carola-Bibiane Schönlieb. Generalized Lie symmetries in physics-informed neural operators. *arXiv preprint arXiv:2502.00373*, 2025.

Rui Wang, Robin Walters, and Rose Yu. Incorporating symmetry into deep dynamics models for improved generalization. *arXiv preprint arXiv:2002.03061*, 2020.

Maurice Weiler, Mario Geiger, Max Welling, Wouter Boomsma, and Taco S Cohen. 3D steerable CNNs: Learning rotationally equivariant features in volumetric data. *Advances in Neural Information Processing Systems*, 31, 2018a.

Maurice Weiler, Fred A Hamprecht, and Martin Storath. Learning steerable filters for rotation equivariant CNNs. In *Proceedings of the IEEE Conference on Computer Vision and Pattern Recognition*, pp. 849–858, 2018b.

Jianke Yang, Robin Walters, Nima Dehmamy, and Rose Yu. Generative adversarial symmetry discovery. In *International Conference on Machine Learning*, pp. 39488–39508. PMLR, 2023.

Jianke Yang, Nima Dehmamy, Robin Walters, and Rose Yu. Latent space symmetry discovery. In *International Conference on Machine Learning*, pp. 56047–56070. PMLR, 2024a.

Jianke Yang, Wang Rao, Nima Dehmamy, Robin Walters, and Rose Yu. Symmetry-informed governing equation discovery. *Advances in Neural Information Processing Systems*, 37:65297–65327, 2024b.

Jianke Yang, Manu Bhat, Bryan Hu, Yadi Cao, Nima Dehmamy, Robin Walters, and Rose Yu. Discovering symbolic differential equations with symmetry invariants. *arXiv preprint arXiv:2505.12083*, 2025.

Manzil Zaheer, Satwik Kottur, Siamak Ravanbakhsh, Barnabas Poczos, Russ R Salakhutdinov, and Alexander J Smola. Deep sets. *Advances in Neural Information Processing Systems*, 30, 2017.

Zhi-Yong Zhang, Hui Zhang, Li-Sheng Zhang, and Lei-Lei Guo. Enforcing continuous symmetries in physics-informed neural network for solving forward and inverse problems of partial differential equations. *Journal of Computational Physics*, 492:112415, 2023.

CONTENTS

1 Introduction **1**

2 Related Work **2**

3 Preliminary **3**

4 Method **3**

4.1 Calculation of Differential Invariants 4

4.2 Governing Equation Discovery Based on Differential Invariants 5

4.3 Example Algorithm: DI-SINDy 6

5 Experiment **6**

5.1 Experimental Setup 6

5.2 Quantitative Metrics and Result Analysis 7

5.3 Robust Analysis Against Dataset and Infinitesimal Generator Noise 9

5.4 High-Dimensional Case with Unknown Symmetries: Governing Equation Discovery for Reaction-Diffusion System 9

5.5 Differential Invariants as a Plug-and-Play Module for Equation Discovery 9

6 Conclusion **9**

A Applications of Symmetry **16**

B Preliminary **16**

C Example **17**

D Detailed Calculation Steps of Differential Invariants **18**

D.1 KdV, KS, and Burgers Equations 18

D.2 nKdV Equation 19

E Example Algorithm: DI-SINDy **20**

F Data Generation **20**

G Implementation Detail **20**

H Additional Experiment **20**

H.1 Robustness Analysis Against Dataset Noise 20

H.2 Robustness Analysis Against Infinitesimal Generator Noise 21

H.3 High-Dimensional Case with Unknown Symmetries: Governing Equation Discovery for Reaction-Diffusion System 23

H.4 Differential Invariants as a Plug-and-Play Module for Equation Discovery 27

I Discussion and Limitation **29**

I.1 Dependence on Symmetry Prior 29

I.2 Selection of Prolongation Order 29

I.3 System Discoverability and the Role of Symmetry 30

I.4 Computational Cost 30

A Applications of Symmetry

Symmetry plays an important role in both traditional mathematical physics problems and the field of deep learning. For the mathematical solution of differential equations, symmetry can guide variable substitutions to reduce their order (Olver, 1993; McLachlan, 1995; Ibragimov, 1999; Hydon, 2000; Bluman & Anco, 2008; Bluman, 2010). In recent years, equivariant networks have incorporated symmetry into network architectures, significantly improving performance and generalization in specific scientific and computer vision tasks (Zaheer et al., 2017; Weiler et al., 2018b;a; Kondor & Trivedi, 2018; Wang et al., 2020; Finzi et al., 2021; Satorras et al., 2021; Ruhe et al., 2023; Li et al., 2024; 2025; Hu et al., 2025c). Additionally, symmetry has been introduced into Physics-Informed Neural Networks (PINNs) or used to guide data augmentation to enhance the accuracy of neural PDE solvers (Arora et al., 2024; Lagrave & Tron, 2022; Shumaylov et al., 2024; Li et al., 2022; Zhang et al., 2023; Wang et al., 2025; Akhound-Sadegh et al., 2023; Brandstetter et al., 2022a). Notably, our goal is to discover explicit equations rather than using PINNs to learn the evolution process of PDEs, which means the problem we focus on differs from that of neural PDE solvers.

Yang et al. (2025) is a concurrent work that also proposes discovering symbolic differential equations via symmetry invariants. As independently developed efforts, direct comparison is not strictly necessary. Nevertheless, we provide a detailed analysis to clarify the distinct technical contributions and experimental scope of each approach:

1. **Experimental scope.** The experiments in Yang et al. (2025) consider only simple symmetry groups such as $\mathrm{SO}(2)$. In contrast, our experiments cover a variety of complex Lie groups involving nonlinear infinitesimal generators (See Table 2 for more details).
2. **Unknown symmetry handling.** Yang et al. (2025) consider only the scenario where symmetries are known a priori. We additionally demonstrate a complete end-to-end pipeline that combines our method with the explicit symmetry discovery approach LieNLSD (Hu et al., 2025a) to handle systems with unknown symmetries. For the reaction-diffusion system, Yang et al. (2025) use only the generator $-v\partial_u + u\partial_v$ of unclear origin, whereas we derive a more complete set of five generators as shown in Equation (37) from the output of LieNLSD, reducing the search space to 4 candidate terms versus their 6—yielding a more concise and efficient treatment.
3. **Computation of differential invariants.** Yang et al. (2025) adopt a recursive approach to compute higher-order differential invariants, which incurs significant overhead when the prolongation order is large and introduces instability from the selection of zeroth-order invariants. We directly compute differential invariants of arbitrary order from the infinitesimal generators using characteristic equations, which is more efficient and stable.
4. **Evaluation metrics.** For Transformer-based experiments, Yang et al. (2025) evaluate using $\mathcal{C}$, SP, and PE, whereas we follow E2E (Kamienny et al., 2022) in using R^2 and Acc_τ, making a direct numerical comparison uninformative.

B Preliminary

We briefly present some preliminary knowledge concerning partial differential equations and their Lie point symmetries. For more details, please refer to the textbook (Olver, 1993).

Partial differential equations. Let the independent variable $x \in X = \mathbb{R}^p$ and the dependent variable $u \in U = \mathbb{R}^q$. We denote the k-th order derivative of u with respect to x as $u^\alpha_J = \frac{\partial^k u^\alpha}{\partial x^{j_1} \partial x^{j_2} \dots \partial x^{j_k}} \in U_k$, where $\alpha \in \{1, \dots, q\}$, $J = (j_1, \dots, j_k)$, and $j_i \in \{1, \dots, p\}$. Furthermore, all derivatives of u with respect to x up to order n are denoted as $u^{(n)} \in U^{(n)} = U \times U_1 \times \cdots \times U_n$. Based on the above concepts, we can define a system of n-th order partial differential equations as $F(x, u^{(n)}) = 0$, where $F : X \times U^{(n)} \to \mathbb{R}^l$. Its solution is given by a smooth function $f : X \to U$.

Lie point symmetries. The solution to the system of partial differential equations $F(x, u^{(n)}) = 0$ can also be represented by the graph $\Gamma_f = \{(x, f(x)) : x \in X\}$ of the function $f : X \to U$. Let the Lie group G act on $X \times U$. We say that G is a symmetry group of $F(x, u^{(n)}) = 0$ if, for any solution

f with its graph Γ_f and any group element $g \in G$, $g \cdot \Gamma_f = \{(\tilde{x}, \tilde{u}) = g \cdot (x, u) : (x, u) \in \Gamma_f\}$ is the graph $\Gamma_{\tilde{f}}$ of another solution $\tilde{f}$.

The Lie point symmetries of partial differential equations can be restated more simply if we introduce the concept of the prolonged group action, which acts on $X \times U^{(n)}$. Denote the action of a group element $g \in G$ at a point $(x, u) \in X \times U$ as $(\tilde{x}, \tilde{u}) = g \cdot (x, u)$. Then, we define the n-th order prolongation of g at the point $(x, u^{(n)}) \in X \times U^{(n)}$ as $\mathrm{pr}^{(n)} g \cdot (x, u^{(n)}) = (\tilde{x}, \tilde{u}^{(n)})$, where $\tilde{u}^{(n)}$ consists of all derivatives of $\tilde{u}$ with respect to $\tilde{x}$ up to order n. G is a symmetry group of $F(x, u^{(n)}) = 0$ means that for any solution $u = f(x)$ and any group element $g \in G$, $F(\mathrm{pr}^{(n)} g \cdot (x, u^{(n)})) = 0$ holds.

Infinitesimal criteria. Suppose the Lie group G corresponds to the Lie algebra $\mathfrak{g}$, which can be associated via the exponential map $\exp : \mathfrak{g} \to G$. The infinitesimal group action $\mathbf{v} \in \mathfrak{g}$ at the point $(x, u) \in X \times U$ is defined as $\mathbf{v}|_{(x,u)} = \frac{\mathrm{d}}{\mathrm{d}\epsilon}\big|_{\epsilon=0} [\exp(\epsilon \mathbf{v}) \cdot (x, u)]$. Note that $\mathbf{v}$ is expressed in terms of the partial differential operator ∇ as its special basis, which indicates that it can directly act on functions defined on $X \times U$. Taking the $\mathrm{SO}(2)$ group $\epsilon \cdot (x, u) = (x \cos\epsilon - u \sin\epsilon, x \sin\epsilon + u \cos\epsilon)$ as an example, its infinitesimal group action is $\mathbf{v}|_{(x,u)} = -u \frac{\partial}{\partial x} + x \frac{\partial}{\partial u}$.

Similarly, we define the n-th order prolongation of $\mathbf{v} \in \mathfrak{g}$ at the point $(x, u^{(n)}) \in X \times U^{(n)}$ as $\mathrm{pr}^{(n)} \mathbf{v}\big|_{(x,u^{(n)})} = \frac{\mathrm{d}}{\mathrm{d}\epsilon}\big|_{\epsilon=0} \left\{\mathrm{pr}^{(n)} [\exp(\epsilon \mathbf{v})] \cdot (x, u^{(n)})\right\}$. Then, according to Theorem 2.31 in the textbook (Olver, 1993), G is a symmetry group of $F(x, u^{(n)}) = 0$ if, for every $\mathbf{v} \in \mathfrak{g}$, $\mathrm{pr}^{(n)} \mathbf{v} \left[F(x, u^{(n)})\right] = 0$ whenever $F(x, u^{(n)}) = 0$.

C EXAMPLE

We take the KdV equation $u_t + u u_x + u_{xxx} = 0$ as an example to intuitively understand the concepts introduced in Section B. In this case, the independent variables are $(x, t) \in X = \mathbb{R}^2$, and the dependent variable is $u \in U = \mathbb{R}$. Consider the group G acting on $X \times U$, which includes three types of group actions:

$$\begin{cases} \epsilon_1 \cdot (x, t, u) = (x + \epsilon_1, t, u), \\ \epsilon_2 \cdot (x, t, u) = (x, t + \epsilon_2, u), \\ \epsilon_3 \cdot (x, t, u) = (x + \epsilon_3 t, t, u + \epsilon_3). \end{cases} \tag{11}$$

According to the definition $\mathbf{v}|_{(x,u)} = \frac{\mathrm{d}}{\mathrm{d}\epsilon}\big|_{\epsilon=0} [\exp(\epsilon \mathbf{v}) \cdot (x, u)]$, the infinitesimal generators are:

$$\begin{cases} \mathbf{v}_1 = \frac{\partial}{\partial x}, \\ \mathbf{v}_2 = \frac{\partial}{\partial t}, \\ \mathbf{v}_3 = t \frac{\partial}{\partial x} + \frac{\partial}{\partial u}. \end{cases} \tag{12}$$

Assuming $u = f(x, t)$ is a solution to the KdV equation, then under the aforementioned three types of group actions, the graph $\Gamma_f = \{(x, t, f(x, t)) : (x, t) \in X\}$ is transformed into the graphs of the following three functions, respectively:

$$\begin{cases} u^{(1)} = f(x - \epsilon_1, t), \\ u^{(2)} = f(x, t - \epsilon_2), \\ u^{(3)} = f(x - \epsilon_3 t, t) + \epsilon_3. \end{cases} \tag{13}$$

It is easy to verify that if $u = f(x, t)$ satisfies the KdV equation, then $u^{(1)}, u^{(2)}, u^{(3)}$ are also solutions of the equation. Therefore, we call G the symmetry group of the KdV equation.

Note that $u_t^{(3)} = -\epsilon_3 f_x(x - \epsilon_3 t, t) + f_t(x - \epsilon_3 t, t)$. The forms of the other transformed derivatives remain unchanged. Then, we can provide the prolongation of group actions:

$$\begin{cases} \mathrm{pr}^{(n)} \epsilon_1 \cdot (x, t, u, u_t, u_x, \dots) = (x + \epsilon_1, t, u, u_t, u_x, \dots), \\ \mathrm{pr}^{(n)} \epsilon_2 \cdot (x, t, u, u_t, u_x, \dots) = (x, t + \epsilon_2, u, u_t, u_x, \dots), \\ \mathrm{pr}^{(n)} \epsilon_3 \cdot (x, t, u, u_t, u_x, \dots) = (x + \epsilon_3 t, t, u + \epsilon_3, -\epsilon_3 u_x + u_t, u_x, \dots). \end{cases} \tag{14}$$

According to the definition $\mathrm{pr}^{(n)}\mathbf{v}\big|_{(x,u^{(n)})} = \frac{\mathrm{d}}{\mathrm{d}\epsilon}\big|_{\epsilon=0}\left\{\mathrm{pr}^{(n)}\left[\exp(\epsilon\mathbf{v})\right]\cdot(x,u^{(n)})\right\}$, the prolongation of the infinitesimal generators are:

$$\begin{cases}\mathrm{pr}^{(n)}\mathbf{v}_1 = \frac{\partial}{\partial x},\\ \mathrm{pr}^{(n)}\mathbf{v}_2 = \frac{\partial}{\partial t},\\ \mathrm{pr}^{(n)}\mathbf{v}_3 = t\frac{\partial}{\partial x} + \frac{\partial}{\partial u} - u_x\frac{\partial}{\partial u_t}.\end{cases} \tag{15}$$

Then, we can observe that the infinitesimal criteria $\mathrm{pr}^{(n)}\mathbf{v}_i(u_t+uu_x+u_{xxx}) = 0$ hold for $i = 1, 2, 3$.

D Detailed Calculation Steps of Differential Invariants

Consider the case where $X \times U = \mathbb{R}^2 \times \mathbb{R}$, with $(x, t) \in X$ as the independent variables and $u \in U$ as the dependent variable. We specify the highest prolongation order as $n = 4$, so the initial search space consists of the terms $\{t, x, u, u_t, u_x, u_{xx}, u_{xxx}, u_{xxxx}\}$ (for simplicity, we assume the dynamical system is first-order, meaning the highest-order partial derivative of u with respect to t is first-order).

D.1 KdV, KS, and Burgers Equations

As shown in Table 2, the infinitesimal generators of the symmetry groups for the KdV, KS, and Burgers equations are:

$$\mathbf{v}_1 = \frac{\partial}{\partial x}, \quad \mathbf{v}_2 = \frac{\partial}{\partial t}, \quad \mathbf{v}_3 = t\frac{\partial}{\partial x} + \frac{\partial}{\partial u}. \tag{16}$$

We first compute their fourth-order prolongations. For $\mathrm{pr}^{(4)}\mathbf{v}_1$, we calculate its coefficients from Equation (4):

$$\begin{cases}\phi^t = \mathrm{D}_t(-u_x) + u_{tx} = 0,\\ \phi^x = \mathrm{D}_x(-u_x) + u_{xx} = 0,\\ \phi^{xx} = \mathrm{D}_{xx}(-u_x) + u_{xxx} = 0,\\ \phi^{xxx} = \mathrm{D}_{xxx}(-u_x) + u_{xxxx} = 0,\\ \phi^{xxxx} = \mathrm{D}_{xxxx}(-u_x) + u_{xxxxx} = 0.\end{cases} \tag{17}$$

Therefore, we have:

$$\mathrm{pr}^{(4)}\mathbf{v}_1 = \mathbf{v}_1 = \frac{\partial}{\partial x}. \tag{18}$$

Similarly, it can be obtained that:

$$\mathrm{pr}^{(4)}\mathbf{v}_2 = \mathbf{v}_2 = \frac{\partial}{\partial t}. \tag{19}$$

The coefficients of $\mathrm{pr}^{(4)}\mathbf{v}_3$ are calculated as follows:

$$\begin{cases}\phi^t = \mathrm{D}_t(1 - tu_x) + tu_{tx} = -u_x,\\ \phi^x = \mathrm{D}_x(1 - tu_x) + tu_{xx} = 0,\\ \phi^{xx} = \mathrm{D}_{xx}(1 - tu_x) + tu_{xxx} = 0,\\ \phi^{xxx} = \mathrm{D}_{xxx}(1 - tu_x) + tu_{xxxx} = 0,\\ \phi^{xxxx} = \mathrm{D}_{xxxx}(1 - tu_x) + tu_{xxxxx} = 0.\end{cases} \tag{20}$$

This means:

$$\mathrm{pr}^{(4)}\mathbf{v}_3 = \mathbf{v}_3 - u_x\frac{\partial}{\partial u_t} = t\frac{\partial}{\partial x} + \frac{\partial}{\partial u} - u_x\frac{\partial}{\partial u_t}. \tag{21}$$

Substitute $\mathrm{pr}^{(4)}\mathbf{v}_1$ and $\mathrm{pr}^{(4)}\mathbf{v}_2$ into Equation (5):

$$\frac{\partial\eta}{\partial x} = \frac{\partial\eta}{\partial t} = 0. \tag{22}$$

Therefore, the differential invariants do not contain the terms x and t. The search space can be narrowed down to $\{u, u_t, u_x, u_{xx}, u_{xxx}, u_{xxxx}\}$.

For $\mathrm{pr}^{(4)}\mathbf{v}_3$, we can construct the characteristic equation as shown in Equation (6) (Note that the term x has already been excluded, so the $t\frac{\partial}{\partial x}$ in $\mathrm{pr}^{(4)}\mathbf{v}_3$ can be ignored):

$$\mathrm{d}u = -\frac{\mathrm{d}u_t}{u_x}. \tag{23}$$

By integrating it, we get:

$$u_t + uu_x = c. \tag{24}$$

Replacing u and u_t in the search space with the integration constant $u_t + uu_x$, we obtain the final differential invariants $\{u_t + uu_x, u_x, u_{xx}, u_{xxx}, u_{xxxx}\}$.

D.2 nKdV Equation

The infinitesimal generators of the symmetry group for the nKdV equation are shown in Table 2 as:

$$\mathbf{v}_1 = \frac{\partial}{\partial x}, \quad \mathbf{v}_2 = e^{-\frac{t}{t_0}}\frac{\partial}{\partial t}, \quad \mathbf{v}_3 = t_0(e^{\frac{t}{t_0}} - 1)\frac{\partial}{\partial x} + \frac{\partial}{\partial u}. \tag{25}$$

The form of $\mathrm{pr}^{(4)}\mathbf{v}_1$ is shown in Equation (18). For $\mathrm{pr}^{(4)}\mathbf{v}_2$, we calculate its coefficients based on Equation (4):

$$\begin{cases} \phi^t = \mathrm{D}_t(-e^{-\frac{t}{t_0}}u_t) + e^{-\frac{t}{t_0}}u_{tt} = \frac{u_t}{t_0}e^{-\frac{t}{t_0}}, \\ \phi^x = \mathrm{D}_x(-e^{-\frac{t}{t_0}}u_t) + e^{-\frac{t}{t_0}}u_{tx} = 0, \\ \phi^{xx} = \mathrm{D}_{xx}(-e^{-\frac{t}{t_0}}u_t) + e^{-\frac{t}{t_0}}u_{txx} = 0, \\ \phi^{xxx} = \mathrm{D}_{xxx}(-e^{-\frac{t}{t_0}}u_t) + e^{-\frac{t}{t_0}}u_{txxx} = 0, \\ \phi^{xxxx} = \mathrm{D}_{xxxx}(-e^{-\frac{t}{t_0}}u_t) + e^{-\frac{t}{t_0}}u_{txxxx} = 0. \end{cases} \tag{26}$$

Then, we have:

$$\mathrm{pr}^{(4)}\mathbf{v}_2 = \mathbf{v}_2 + \frac{u_t}{t_0}e^{-\frac{t}{t_0}}\frac{\partial}{\partial u_t} = e^{-\frac{t}{t_0}}\frac{\partial}{\partial t} + \frac{u_t}{t_0}e^{-\frac{t}{t_0}}\frac{\partial}{\partial u_t}. \tag{27}$$

For $\mathrm{pr}^{(4)}\mathbf{v}_3$, its coefficients are:

$$\begin{cases} \phi^t = \mathrm{D}_t[1 - t_0(e^{\frac{t}{t_0}} - 1)u_x] + t_0(e^{\frac{t}{t_0}} - 1)u_{tx} = -u_x e^{\frac{t}{t_0}}, \\ \phi^x = \mathrm{D}_x[1 - t_0(e^{\frac{t}{t_0}} - 1)u_x] + t_0(e^{\frac{t}{t_0}} - 1)u_{xx} = 0, \\ \phi^{xx} = \mathrm{D}_{xx}[1 - t_0(e^{\frac{t}{t_0}} - 1)u_x] + t_0(e^{\frac{t}{t_0}} - 1)u_{xxx} = 0, \\ \phi^{xxx} = \mathrm{D}_{xxx}[1 - t_0(e^{\frac{t}{t_0}} - 1)u_x] + t_0(e^{\frac{t}{t_0}} - 1)u_{xxxx} = 0, \\ \phi^{xxxx} = \mathrm{D}_{xxxx}[1 - t_0(e^{\frac{t}{t_0}} - 1)u_x] + t_0(e^{\frac{t}{t_0}} - 1)u_{xxxxx} = 0. \end{cases} \tag{28}$$

Then, we get:

$$\mathrm{pr}^{(4)}\mathbf{v}_3 = \mathbf{v}_3 - u_x e^{\frac{t}{t_0}}\frac{\partial}{\partial u_t} = t_0(e^{\frac{t}{t_0}} - 1)\frac{\partial}{\partial x} + \frac{\partial}{\partial u} - u_x e^{\frac{t}{t_0}}\frac{\partial}{\partial u_t}. \tag{29}$$

Similarly to Equation (22), we exclude the variable x based on $\mathrm{pr}^{(4)}\mathbf{v}_1$ and update the search space as $\{t, u, u_t, u_x, u_{xx}, u_{xxx}, u_{xxxx}\}$.

Construct the characteristic equation as shown in Equation (6) based on $\mathrm{pr}^{(4)}\mathbf{v}_2$:

$$e^{\frac{t}{t_0}}\mathrm{d}t = \frac{t_0}{u_t}e^{\frac{t}{t_0}}\mathrm{d}u_t. \tag{30}$$

Integrating it yields the general solution:

$$e^{-\frac{t}{t_0}}u_t = c. \tag{31}$$

By replacing the terms t and u_t with integral constants, we update the search space as $\{e^{-\frac{t}{t_0}}u_t, u, u_x, u_{xx}, u_{xxx}, u_{xxxx}\}$.

For $\mathrm{pr}^{(4)}\mathbf{v}_3$, we construct the characteristic equation as:

$$\mathrm{d}u = -\frac{1}{u_x}e^{-\frac{t}{t_0}}\mathrm{d}u_t. \tag{32}$$

Integral yields:

$$e^{-\frac{t}{t_0}}u_t + uu_x = c. \tag{33}$$

Introducing it into the search space to replace $e^{-\frac{t}{t_0}}u_t$ and u, we obtain the final differential invariants as $\{e^{-\frac{t}{t_0}}u_t + uu_x, u_x, u_{xx}, u_{xxx}, u_{xxxx}\}$.

E EXAMPLE ALGORITHM: DI-SINDY

Algorithm 1 DI-SINDy (SINDy based on Differential Invariants)

Input: Dataset $\mathcal{D} = \{(x[i], u[i])\}_{i=1}^{N}$, prolongation order n, infinitesimal generators of the symmetry group $V(\mathfrak{g}) = \{\mathbf{v}_1, \dots, \mathbf{v}_r\}$.
Output: Explicit governing equation $F(x, u^{(n)}) = 0$.
Execute:
Estimate the derivatives of u with respect to x using the central difference method, resulting in the prolonged dataset $\mathrm{pr}^{(n)}\mathcal{D} = \{(x[i], u^{(n)}[i])\}_{i=1}^{N}$.
if $V(\mathfrak{g}) = \emptyset$ **then**
  Use the method of symmetry discovery to obtain the infinitesimal generators $V(\mathfrak{g}) = \{\mathbf{v}_1, \dots, \mathbf{v}_r\}$ of the symmetry group from $\mathrm{pr}^{(n)}\mathcal{D}$.
end if
Derive the prolonged infinitesimal generators $\{\mathrm{pr}^{(n)}\mathbf{v}_1, \dots, \mathrm{pr}^{(n)}\mathbf{v}_r\}$ according to Equations (2) to (4).
Compute differential invariants $\{\eta^1(x, u^{(n)}), \dots, \eta^k(x, u^{(n)})\}$ according to Equations (5) to (7).
For the equation skeleton $\eta^k(x, u^{(n)}) = W\Theta(\eta^1(x, u^{(n)}), \dots, \eta^{k-1}(x, u^{(n)}))$, optimize the coefficient matrix W using SINDy based on $\mathrm{pr}^{(n)}\mathcal{D}$.
Return $F(x, u^{(n)}) = \eta^k(x, u^{(n)}) - W\Theta(\eta^1(x, u^{(n)}), \dots, \eta^{k-1}(x, u^{(n)})) = 0$.

F DATA GENERATION

For the generation of the dataset, we follow the setup of Ko et al. (2024), which we restate as follows. In the Burgers equation, $\nu = 0.01$, and in the nKdV equation, $t_0 = 50$. For a one-dimensional PDE $u_t = f(x, t, u, u_x, u_{xx}, \dots)$ defined on $x \in [0, L]$, the initial condition $u(x, t = 0)$ is generated by randomly sampling the coefficients A_p, l_p, ϕ_p of the Fourier series $u(x, t = 0) = \sum_{p=1}^{P} A_p \sin(2\pi l_p x/L + \phi_p)$. Then, the spatial derivatives of u with respect to x are estimated using the pseudospectral method, and the temporal evolution u_t is computed from the explicit expression of the equation. After numerically integrating the PDE over $t \in [0, T]$ using an ODE solver, we obtain $N_x \times N_t$ discrete grid points on $[0, L] \times [0, T]$, where $N_x = 256$ and $N_t = 140$. Specifically, the dataset $u(x, t)$ for the Burgers equation is solved indirectly via the heat equation $\phi_t = \phi_{xx}$, which are related through the Cole-Hopf transformation $u = 2\nu \frac{\partial}{\partial x} \ln \phi$. We add multiplicative noise $u' = u \cdot (1 + \epsilon)$ to the vector field u to simulate real-world perturbations, where $\epsilon \sim \mathcal{N}(0, \sigma^2)$. We set the noise level $\sigma = 10^{-2}$ for the KdV and nKdV equations, $\sigma = 10^{-3}$ for Burgers equation, and $\sigma = 10^{-4}$ for the KS equation.

G IMPLEMENTATION DETAIL

We select trajectory samples generated from 4 initial conditions in the training dataset for equation discovery and use the L-BFGS optimizer with a learning rate of 0.1 for training. During sparse regression, parameters smaller than the threshold are masked to 0 upon convergence, and the optimizer is reset. For the KdV, KS, and nKdV equations, we set the threshold to 0.5, while for Burgers equation, we set it to 5×10^{-3}. All methods share the above experimental settings to ensure a fair comparison. We perform experiments on a single-core NVIDIA GeForce RTX 3090 GPU with available memory of $24,576$ MiB.

H ADDITIONAL EXPERIMENT

H.1 ROBUSTNESS ANALYSIS AGAINST DATASET NOISE

Taking the Burgers equation as an example, we evaluate the robustness of DI-SINDy under increasing dataset noise levels. Note that, as mentioned in Appendix F, the main results of the Burgers equation in Section 5.2 are obtained under a dataset noise level of $\sigma = 10^{-3}$. Here, we further increase the

Table 4: Success rates and RMSE of SINDy and DI-SINDy (Ours) for the Burgers equation with different dataset noise levels. All experimental results are averaged over 50 runs. RMSE is presented in the format of mean ± std.

Dataset noise level	Method	Success rate (↑)	RMSE (successful) (↓)	RMSE (all) (↓)
$\sigma = 10^{-3}$	SINDy	4%	$(2.11 \pm 0.14) \times 10^{-2}$	$(1.52 \pm 2.34) \times 10^{-1}$
	DI-SINDy (Ours)	**98%**	$\mathbf{(2.66 \pm 1.32) \times 10^{-4}}$	$\mathbf{(4.02 \pm 9.62) \times 10^{-4}}$
$\sigma = 3 \times 10^{-3}$	SINDy	0%	N/A	$(3.13 \pm 2.23) \times 10^{-1}$
	DI-SINDy (Ours)	**100%**	$\mathbf{(2.14 \pm 0.50) \times 10^{-3}}$	$\mathbf{(2.14 \pm 0.50) \times 10^{-3}}$
$\sigma = 5 \times 10^{-3}$	SINDy	0%	N/A	$(3.07 \pm 1.86) \times 10^{-1}$
	DI-SINDy (Ours)	**28%**	$\mathbf{(3.18 \pm 0.28) \times 10^{-3}}$	$\mathbf{(5.98 \pm 1.75) \times 10^{-3}}$

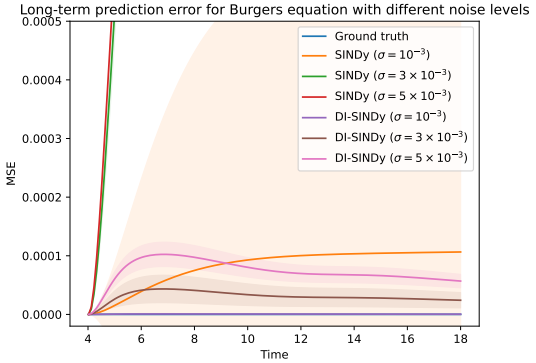

Figure 4: Long-term prediction errors of SINDy and DI-SINDy (Ours) for the Burgers equation with different dataset noise levels. The MSE at each time step is averaged over 4 initial conditions and 50 runs, with the shaded area representing the standard deviation.

dataset noise level to $\sigma = \{3 \times 10^{-3}, 5 \times 10^{-3}\}$. The corresponding success rates and RMSE of DI-SINDy and SINDy are shown in Table 4, while the long-term prediction errors are illustrated in Figure 4. It is noted that DI-SINDy ($\sigma = 10^{-3}$) exhibits a sufficiently small deviation from ground truth compared to other settings, such that their error curves almost overlap under the coordinate scale of Figure 4. As the dataset noise level increases, SINDy fails completely, whereas our DI-SINDy maintains a certain success rate and high accuracy, which demonstrates its stronger robustness against real-world disturbances.

H.2 Robustness Analysis Against Infinitesimal Generator Noise

Sometimes we cannot obtain a perfectly accurate symmetry group because our prior knowledge of the scientific problem is biased, or there are errors in the symmetry discovery method. Therefore, we further discuss the robustness of DI-SINDy with respect to noise in the infinitesimal generators. Taking the Burgers equation as an example again, we assume that the last infinitesimal generator is inaccurate: $\mathbf{v}_3 = (1+\delta)t\frac{\partial}{\partial x} + \frac{\partial}{\partial u}$. Note that numerical perturbations on $\mathbf{v}_1 = (1+\delta)\frac{\partial}{\partial x}$ or $\mathbf{v}_2 = (1+\delta)\frac{\partial}{\partial t}$ do not affect the results, as they are equivalent as "bases" up to a constant factor. Then, similar to Equation (21), we obtain its prolongation:

$$\mathrm{pr}^{(4)}\mathbf{v}_3 = (1+\delta)t\frac{\partial}{\partial x} + \frac{\partial}{\partial u} - (1+\delta)u_x\frac{\partial}{\partial u_t}. \tag{34}$$

The characteristic equation (23) becomes:

$$\mathrm{d}u = -\frac{\mathrm{d}u_t}{(1+\delta)u_x}. \tag{35}$$

Integrating, we obtain the biased differential invariants as $\{u_t + (1+\delta)uu_x, u_x, u_{xx}, u_{xxx}, u_{xxxx}\}$.

Table 5: Success rates and RMSE of different SINDy-based methods with varying infinitesimal generator noise levels for the Burgers equation. All experimental results are averaged over 50 runs. RMSE is presented in the format of mean ± std.

Method	Infinitesimal generator noise level	Success rate (↑)	RMSE (successful) (↓)	RMSE (all) (↓)
SINDy	N/A	4%	$(2.11 \pm 0.14) \times 10^{-2}$	$(1.52 \pm 2.34) \times 10^{-1}$
EquivSINDy-r ($\lambda = 10^{-3}$)	$\delta = 10^{-1}$	28%	$(8.89 \pm 2.52) \times 10^{-3}$	$(1.30 \pm 3.66) \times 10^{-1}$
EquivSINDy-r ($\lambda = 10^{-2}$)		58%	$(4.54 \pm 0.66) \times 10^{-2}$	$(1.37 \pm 3.77) \times 10^{-1}$
EquivSINDy-r ($\lambda = 10^{-1}$)		82%	$(6.75 \pm 0.07) \times 10^{-2}$	$(1.61 \pm 3.79) \times 10^{-1}$
DI-SINDy (Ours)		**100%**	$\mathbf{(2.16 \pm 1.16) \times 10^{-4}}$	$\mathbf{(2.16 \pm 1.16) \times 10^{-4}}$
EquivSINDy-r ($\lambda = 10^{-3}$)	$\delta = 3 \times 10^{-1}$	36%	$(3.08 \pm 1.22) \times 10^{-2}$	$(1.94 \pm 4.04) \times 10^{-1}$
EquivSINDy-r ($\lambda = 10^{-2}$)		40%	$(1.51 \pm 0.11) \times 10^{-1}$	$(1.75 \pm 1.18) \times 10^{-1}$
EquivSINDy-r ($\lambda = 10^{-1}$)		64%	$(2.05 \pm 0.02) \times 10^{-1}$	$(2.82 \pm 3.45) \times 10^{-1}$
DI-SINDy (Ours)		**90%**	$\mathbf{(1.08 \pm 0.24) \times 10^{-3}}$	$\mathbf{(1.09 \pm 0.24) \times 10^{-3}}$
EquivSINDy-r ($\lambda = 10^{-3}$)	$\delta = 5 \times 10^{-1}$	22%	$(5.35 \pm 1.33) \times 10^{-2}$	$(2.19 \pm 4.04) \times 10^{-1}$
EquivSINDy-r ($\lambda = 10^{-2}$)		22%	$(2.54 \pm 0.24) \times 10^{-1}$	$(2.87 \pm 3.15) \times 10^{-1}$
EquivSINDy-r ($\lambda = 10^{-1}$)		54%	$(3.42 \pm 0.04) \times 10^{-1}$	$(3.92 \pm 2.99) \times 10^{-1}$
DI-SINDy (Ours)		**70%**	$\mathbf{(1.94 \pm 0.35) \times 10^{-3}}$	$\mathbf{(1.99 \pm 0.33) \times 10^{-3}}$

In practice, we set different infinitesimal generator noise levels $\delta = \{10^{-1}, 3 \times 10^{-1}, 5 \times 10^{-1}\}$ for EquivSINDy-r and DI-SINDy, respectively, for evaluation. The corresponding success rates and RMSE are presented in Table 5. We note that sometimes EquivSINDy-r with a smaller regularization weight λ exhibits an increase rather than a decrease in success rate as δ increases. This is because it inherently struggles to filter out key terms from the large search space, while the enhanced correlation coefficients of the infinitesimal generators highlight the correct answer. Overall, in most cases, the accuracy of symmetry-informed equation discovery methods decreases as the perturbation magnitude increases, but our DI-SINDy consistently performs better.

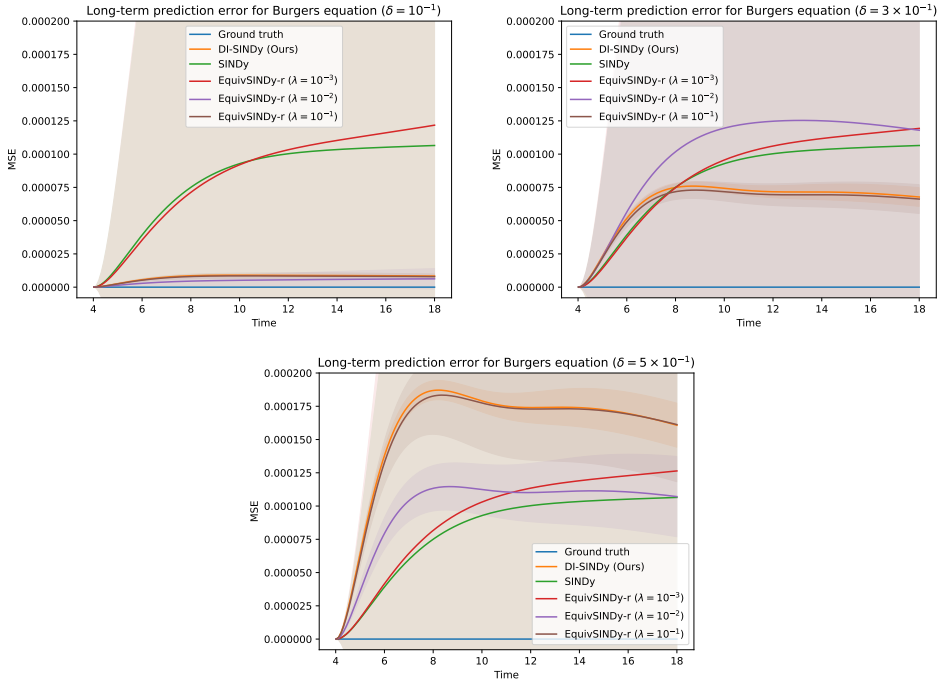

Figure 5: Long-term prediction errors of different SINDy-based methods with varying infinitesimal generator noise levels for the Burgers equation. The MSE at each time step is averaged over 4 initial conditions and 50 runs, with the shaded area representing the standard deviation.

Figure 5 illustrates the variation of long-term prediction errors with respect to δ for different SINDy-based methods. We observe that the results of DI-SINDy and EquivSINDy-r with larger λ are more affected by errors in the infinitesimal generator—this is theoretically reasonable, as they adhere

more strictly to symmetry. Even so, compared to SINDy, which does not incorporate symmetry information, our DI-SINDy achieves more stable long-term prediction results as long as δ does not exceed 3×10^{-1}. This demonstrates that DI-SINDy has a high tolerance for perturbations in the infinitesimal generator, indicating its strong potential for integration with symmetry discovery methods.

H.3 High-Dimensional Case with Unknown Symmetries: Governing Equation Discovery for Reaction-Diffusion System

Furthermore, we attempt to solve the reaction-diffusion system (Champion et al., 2019) using our method, for which the explicit equation is:

$$\begin{cases} u_t = (1-(u^2+v^2))u + \beta(u^2+v^2)v + d_1(u_{xx}+u_{yy}), \\ v_t = -\beta(u^2+v^2)u + (1-(u^2+v^2))v + d_2(v_{xx}+v_{yy}), \end{cases} \tag{36}$$

with $d_1 = 0.1$, $d_2 = 0.1$, and $\beta = 1$. This is a high-dimensional case where both the independent variables $(t, x, y) \in X$ and the dependent variables $(u, v) \in U$ are vectors. The initial terms for its second-order prolongation are $\{t, x, y, u, v, u_x, u_y, v_x, v_y, u_{xx}, u_{xy}, u_{yy}, v_{xx}, v_{xy}, v_{yy}, u_t, v_t\}$. This constitutes a very large search space, and according to the form of Equation (36), we need to extend it to at least third-order terms to include the correct solution, which would undoubtedly overwhelm methods such as SINDy and EquivSINDy-r (as mentioned in the original paper (Yang et al., 2024b), EquivSINDy-r only attempts to operate in the latent space). We will next demonstrate how to address this challenge based on differential invariants.

First, using LieNLSD (Hu et al., 2025a) (a method for explicitly discovering nonlinear symmetries) we can determine that this system possesses spatiotemporal translation and $\mathrm{SO}(2)$ symmetry, with the corresponding infinitesimal generators being (for the detailed symmetry discovery process, please refer to the original paper (Hu et al., 2025a)):

$$\mathbf{v}_1 = -v\frac{\partial}{\partial u} + u\frac{\partial}{\partial v}, \quad \mathbf{v}_2 = -y\frac{\partial}{\partial x} + x\frac{\partial}{\partial y}, \quad \mathbf{v}_3 = \frac{\partial}{\partial t}, \quad \mathbf{v}_4 = \frac{\partial}{\partial x}, \quad \mathbf{v}_5 = \frac{\partial}{\partial y}, \tag{37}$$

where $\{\mathbf{v}_3, \mathbf{v}_4, \mathbf{v}_5\}$ can narrow the search space to $\{u, v, u_x, u_y, v_x, v_y, u_{xx}, u_{xy}, u_{yy}, v_{xx}, v_{xy}, v_{yy}, u_t, v_t\}$. Then we calculate the second-order prolongation of $\{\mathbf{v}_1, \mathbf{v}_2\}$:

$$\begin{cases} \mathrm{pr}^{(2)}\mathbf{v}_1 = & (-v\frac{\partial}{\partial u} + u\frac{\partial}{\partial v}) + (-v_t\frac{\partial}{\partial u_t} + u_t\frac{\partial}{\partial v_t}) + (-v_x\frac{\partial}{\partial u_x} + u_x\frac{\partial}{\partial v_x}) + (-v_y\frac{\partial}{\partial u_y} + u_y\frac{\partial}{\partial v_y}) \\ & +(-v_{xx}\frac{\partial}{\partial u_{xx}} + u_{xx}\frac{\partial}{\partial v_{xx}}) + (-v_{xy}\frac{\partial}{\partial u_{xy}} + u_{xy}\frac{\partial}{\partial v_{xy}}) + (-v_{yy}\frac{\partial}{\partial u_{yy}} + u_{yy}\frac{\partial}{\partial v_{yy}}), \\ \mathrm{pr}^{(2)}\mathbf{v}_2 = & (-y\frac{\partial}{\partial x} + x\frac{\partial}{\partial y}) + (-u_y\frac{\partial}{\partial u_x} + u_x\frac{\partial}{\partial u_y}) + (-v_y\frac{\partial}{\partial v_x} + v_x\frac{\partial}{\partial v_y}) \\ & +(-2u_{xy}\frac{\partial}{\partial u_{xx}} + 2u_{xy}\frac{\partial}{\partial u_{yy}}) + (-2v_{xy}\frac{\partial}{\partial v_{xx}} + 2v_{xy}\frac{\partial}{\partial v_{yy}}) \\ & +(u_{xx}-u_{yy})\frac{\partial}{\partial u_{xy}} + (v_{xx}-v_{yy})\frac{\partial}{\partial v_{xy}}. \end{cases} \tag{38}$$

Construct the characteristic equation based on $\mathrm{pr}^{(2)}\mathbf{v}_1$:

$$\begin{aligned} \frac{\mathrm{d}v}{u} = -\frac{\mathrm{d}u}{v} = \frac{\mathrm{d}v_x}{u_x} = -\frac{\mathrm{d}u_x}{v_x} = \frac{\mathrm{d}v_y}{u_y} = -\frac{\mathrm{d}u_y}{v_y} = \frac{\mathrm{d}v_t}{u_t} = -\frac{\mathrm{d}u_t}{v_t} \\ = \frac{\mathrm{d}v_{xx}}{u_{xx}} = -\frac{\mathrm{d}u_{xx}}{v_{xx}} = \frac{\mathrm{d}v_{xy}}{u_{xy}} = -\frac{\mathrm{d}u_{xy}}{v_{xy}} = \frac{\mathrm{d}v_{yy}}{u_{yy}} = -\frac{\mathrm{d}u_{yy}}{v_{yy}}. \end{aligned} \tag{39}$$

The search space is then updated to $\{u^2+v^2, vu_x - uv_x, uu_x + vv_x, vu_y - uv_y, uu_y + vv_y, vu_{xx} - uv_{xx}, uu_{xx} + vv_{xx}, vu_{xy} - uv_{xy}, uu_{xy} + vv_{xy}, vu_{yy} - uv_{yy}, uu_{yy} + vv_{yy}, vu_t - uv_t, uu_t + vv_t\}$.

These terms transform under $\mathrm{pr}^{(2)}\mathbf{v}_2$ as:

$$\mathrm{pr}^{(2)}\mathbf{v}_2 \begin{bmatrix} u^2+v^2 \\ vu_x - uv_x \\ uu_x + vv_x \\ vu_y - uv_y \\ uu_y + vv_y \\ vu_{xx} - uv_{xx} \\ uu_{xx} + vv_{xx} \\ vu_{xy} - uv_{xy} \\ uu_{xy} + vv_{xy} \\ vu_{yy} - uv_{yy} \\ uu_{yy} + vv_{yy} \\ vu_t - uv_t \\ uu_t + vv_t \end{bmatrix} = \begin{bmatrix} 0 \\ -vu_y + uv_y \\ -uu_y - vv_y \\ vu_x - uv_x \\ uu_x + vv_x \\ -2vu_{xy} + 2uv_{xy} \\ -2uu_{xy} - 2vv_{xy} \\ v(u_{xx} - u_{yy}) - u(v_{xx} - v_{yy}) \\ u(u_{xx} - u_{yy}) + v(v_{xx} - v_{yy}) \\ 2vu_{xy} - 2uv_{xy} \\ 2uu_{xy} + 2vv_{xy} \\ 0 \\ 0 \end{bmatrix}. \tag{40}$$

To ensure invariance under $\mathrm{pr}^{(2)}\mathbf{v}_2$, we obtain the final differential invariants as $\{u^2+v^2, (vu_{xx} - uv_{xx}) + (vu_{yy} - uv_{yy}), (uu_{xx} + vv_{xx}) + (uu_{yy} + vv_{yy}), vu_t - uv_t, uu_t + vv_t\}$.

After all this, we found that the set of differential invariants is extremely concise compared to the original search space. Based on this, DI-SINDy can construct the equation skeleton:

$$\begin{cases} vu_t - uv_t = W_1\Theta_1(u^2+v^2, vu_{xx} - uv_{xx} + vu_{yy} - uv_{yy}, uu_{xx} + vv_{xx} + uu_{yy} + vv_{yy}), \\ uu_t + vv_t = W_2\Theta_2(u^2+v^2, vu_{xx} - uv_{xx} + vu_{yy} - uv_{yy}, uu_{xx} + vv_{xx} + uu_{yy} + vv_{yy}). \end{cases} \tag{41}$$

In practice, we specify that Θ_1 and Θ_2 include terms up to second order, so the number of their terms is 9. On the other hand, if a function library is constructed based on the original search space while including terms up to third order, a rough estimate suggests it would contain hundreds of terms! Therefore, our DI-SINDy is theoretically more effective in handling such high-dimensional scenarios.

We conduct experiments using the dataset constructed in Hu et al. (2025a). The sparse regression threshold is set to 5×10^{-2}, while other settings remain consistent with the main experiments. Since SINDy and EquivSINDy-r break down as mentioned earlier, we only analyze the results of DI-SINDy individually. We sample 10 discovered equations in Table 6. By observing their forms, we can roughly summarize the results as:

$$\begin{cases} vu_t - uv_t = 0.1(vu_{xx} - uv_{xx} + vu_{yy} - uv_{yy}) + (u^2+v^2)^2, \\ uu_t + vv_t = (u^2+v^2) + 0.1(uu_{xx} + vv_{xx} + uu_{yy} + vv_{yy}) - (u^2+v^2)^2. \end{cases} \tag{42}$$

Equivalently:

$$\begin{cases} u_t = (1-(u^2+v^2))u + (u^2+v^2)v + 0.1(u_{xx} + u_{yy}), \\ v_t = -(u^2+v^2)u + (1-(u^2+v^2))v + 0.1(v_{xx} + v_{yy}). \end{cases} \tag{43}$$

Qualitatively, our DI-SINDy has discovered the correct form of the equation! We further present the quantitative results of 50 runs in Table 7. As shown in Table 6, the failure cases are all due to minor coefficient differences in (u^2+v^2) caused by $(u^2+v^2)^2$, but the main forms remain correct. Overall, our DI-SINDy combined with symmetry discovery methods such as LieNLSD (Hu et al., 2025a) demonstrates significant potential for discovering complex PDEs in high-dimensional dynamic systems with unknown symmetries.

Analysis of failure cases. We identify a systematic data bias as the root cause of the 48% success rate: in the reaction-diffusion dataset, the value of u^2+v^2 for data points fluctuates close to 1. This makes it difficult for the sparse regression model to distinguish between the two candidate terms u^2+v^2 and $(u^2+v^2)^2$, leading to random apportionment of their coefficients. This issue is therefore not caused by our method itself; the sampled results in Table 6 confirm that nearly all failure cases stem from this data bias, which further highlights the potential of differential invariants in high-dimensional scenarios.

Evaluation with different symmetry sources. In the main results above, we use ideal symmetries extracted from the visualization output of LieNLSD (Hu et al., 2025a). Here we additionally evaluate

Table 6: Samples of equation discovery results by DI-SINDy for the reaction-diffusion system.

#	Discovered equation
1	$\begin{cases} vu_t - uv_t = -0.0547(u^2+v^2) + 0.1047(vu_{xx} - uv_{xx} + vu_{yy} - uv_{yy}) + 1.0136(u^2+v^2)^2 \\ uu_t + vv_t = +1.0176(u^2+v^2) + 0.1065(uu_{xx} + vv_{xx} + uu_{yy} + vv_{yy}) - 1.0036(u^2+v^2)^2 \end{cases}$
2	$\begin{cases} vu_t - uv_t = +0.1059(vu_{xx} - uv_{xx} + vu_{yy} - uv_{yy}) + 1.0088(u^2+v^2)^2 \\ uu_t + vv_t = +1.0157(u^2+v^2) + 0.1059(uu_{xx} + vv_{xx} + uu_{yy} + vv_{yy}) - 1.0033(u^2+v^2)^2 \end{cases}$
3	$\begin{cases} vu_t - uv_t = -0.0602(u^2+v^2) + 0.1044(vu_{xx} - uv_{xx} + vu_{yy} - uv_{yy}) + 1.0148(u^2+v^2)^2 \\ uu_t + vv_t = +1.0190(u^2+v^2) + 0.1065(uu_{xx} + vv_{xx} + uu_{yy} + vv_{yy}) - 1.0039(u^2+v^2)^2 \end{cases}$
4	$\begin{cases} vu_t - uv_t = +0.1062(vu_{xx} - uv_{xx} + vu_{yy} - uv_{yy}) + 1.0089(u^2+v^2)^2 \\ uu_t + vv_t = +1.0158(u^2+v^2) + 0.1058(uu_{xx} + vv_{xx} + uu_{yy} + vv_{yy}) - 1.0033(u^2+v^2)^2 \end{cases}$
5	$\begin{cases} vu_t - uv_t = -0.0526(u^2+v^2) + 0.1039(vu_{xx} - uv_{xx} + vu_{yy} - uv_{yy}) + 1.0130(u^2+v^2)^2 \\ uu_t + vv_t = +1.0167(u^2+v^2) + 0.1062(uu_{xx} + vv_{xx} + uu_{yy} + vv_{yy}) - 1.0034(u^2+v^2)^2 \end{cases}$
6	$\begin{cases} vu_t - uv_t = -0.0607(u^2+v^2) + 0.1048(vu_{xx} - uv_{xx} + vu_{yy} - uv_{yy}) + 1.0148(u^2+v^2)^2 \\ uu_t + vv_t = +1.0191(u^2+v^2) + 0.1066(uu_{xx} + vv_{xx} + uu_{yy} + vv_{yy}) - 1.0039(u^2+v^2)^2 \end{cases}$
7	$\begin{cases} vu_t - uv_t = -0.0551(u^2+v^2) + 0.1037(vu_{xx} - uv_{xx} + vu_{yy} - uv_{yy}) + 1.0136(u^2+v^2)^2 \\ uu_t + vv_t = +1.0175(u^2+v^2) + 0.1064(uu_{xx} + vv_{xx} + uu_{yy} + vv_{yy}) - 1.0036(u^2+v^2)^2 \end{cases}$
8	$\begin{cases} vu_t - uv_t = +0.1052(vu_{xx} - uv_{xx} + vu_{yy} - uv_{yy}) + 1.0079(u^2+v^2)^2 \\ uu_t + vv_t = +1.0133(u^2+v^2) + 0.1052(uu_{xx} + vv_{xx} + uu_{yy} + vv_{yy}) - 1.0029(u^2+v^2)^2 \end{cases}$
9	$\begin{cases} vu_t - uv_t = -0.0558(u^2+v^2) + 0.1046(vu_{xx} - uv_{xx} + vu_{yy} - uv_{yy}) + 1.0138(u^2+v^2)^2 \\ uu_t + vv_t = +1.0179(u^2+v^2) + 0.1065(uu_{xx} + vv_{xx} + uu_{yy} + vv_{yy}) - 1.0036(u^2+v^2)^2 \end{cases}$
10	$\begin{cases} vu_t - uv_t = +0.1058(vu_{xx} - uv_{xx} + vu_{yy} - uv_{yy}) + 1.0075(u^2+v^2)^2 \\ uu_t + vv_t = +1.0127(u^2+v^2) + 0.1051(uu_{xx} + vv_{xx} + uu_{yy} + vv_{yy}) - 1.0028(u^2+v^2)^2 \end{cases}$

Table 7: Success rate and RMSE of DI-SINDy for the reaction-diffusion system. Experimental results are averaged over 50 runs. RMSE is presented in the format of mean $\pm$ std.

Success rate (↑)	RMSE (successful) (↓)	RMSE (all) (↓)
48%	$(8.35 \pm 0.59) \times 10^{-3}$	$(9.53 \pm 1.26) \times 10^{-3}$

two settings: (1) approximate symmetries obtained directly from the numerical output of LieNLSD, and (2) approximate symmetries from LieGAN (Yang et al., 2023). The Grassmann distance between the discovered and ground-truth generators for each method is shown in Table 8, confirming that LieNLSD produces significantly more accurate symmetry estimates than LieGAN.

Table 8: Grassmann distance between the discovered and ground-truth symmetry generators of the reaction-diffusion system. Results are restated from Table 5 of Hu et al. (2025a).

Model	Grassmann distance (↓)
LieNLSD (Hu et al., 2025a)	$\mathbf{(1.24 \pm 0.18) \times 10^{-1}}$
LieGAN (Yang et al., 2023)	1.11 ± 0.11

The approximate symmetries correspond to small perturbations of the ideal $\mathrm{SO}(2)$ generators. Specifically, the perturbed generators take the form:

$$\mathbf{v}_1' = -(1+\delta_1)v\frac{\partial}{\partial u} + u\frac{\partial}{\partial v}, \quad \mathbf{v}_2' = -(1+\delta_2)y\frac{\partial}{\partial x} + x\frac{\partial}{\partial y}, \tag{44}$$

for small $\delta_1, \delta_2 \approx 0$. We now derive the perturbed differential invariants, following the same procedure as the ideal case above. Computing the second-order prolongations:

$$\begin{cases} \mathrm{pr}^{(2)}\mathbf{v}_1' = & \left[-(1+\delta_1)v\frac{\partial}{\partial u} + u\frac{\partial}{\partial v}\right] + \left[-(1+\delta_1)v_t\frac{\partial}{\partial u_t} + u_t\frac{\partial}{\partial v_t}\right] \\ & + \left[-(1+\delta_1)v_x\frac{\partial}{\partial u_x} + u_x\frac{\partial}{\partial v_x}\right] + \left[-(1+\delta_1)v_y\frac{\partial}{\partial u_y} + u_y\frac{\partial}{\partial v_y}\right] \\ & + \left[-(1+\delta_1)v_{xx}\frac{\partial}{\partial u_{xx}} + u_{xx}\frac{\partial}{\partial v_{xx}}\right] + \left[-(1+\delta_1)v_{xy}\frac{\partial}{\partial u_{xy}} + u_{xy}\frac{\partial}{\partial v_{xy}}\right] \\ & + \left[-(1+\delta_1)v_{yy}\frac{\partial}{\partial u_{yy}} + u_{yy}\frac{\partial}{\partial v_{yy}}\right], \\ \mathrm{pr}^{(2)}\mathbf{v}_2' = & \left[-(1+\delta_2)y\frac{\partial}{\partial x} + x\frac{\partial}{\partial y}\right] \\ & + \left[-u_y\frac{\partial}{\partial u_x} + (1+\delta_2)u_x\frac{\partial}{\partial u_y}\right] + \left[-v_y\frac{\partial}{\partial v_x} + (1+\delta_2)v_x\frac{\partial}{\partial v_y}\right] \\ & + \left[-2u_{xy}\frac{\partial}{\partial u_{xx}} + 2(1+\delta_2)u_{xy}\frac{\partial}{\partial u_{yy}}\right] + \left[-2v_{xy}\frac{\partial}{\partial v_{xx}} + 2(1+\delta_2)v_{xy}\frac{\partial}{\partial v_{yy}}\right] \\ & + \left[(1+\delta_2)u_{xx} - u_{yy}\right]\frac{\partial}{\partial u_{xy}} + \left[(1+\delta_2)v_{xx} - v_{yy}\right]\frac{\partial}{\partial v_{xy}}. \end{cases} \tag{45}$$

Constructing the characteristic equation based on $\mathrm{pr}^{(2)}\mathbf{v}_1'$:

$$\begin{aligned} \frac{\mathrm{d}v}{u} = -\frac{\mathrm{d}u}{(1+\delta_1)v} = \frac{\mathrm{d}v_x}{u_x} = -\frac{\mathrm{d}u_x}{(1+\delta_1)v_x} = \frac{\mathrm{d}v_y}{u_y} = -\frac{\mathrm{d}u_y}{(1+\delta_1)v_y} = \frac{\mathrm{d}v_t}{u_t} = -\frac{\mathrm{d}u_t}{(1+\delta_1)v_t} \\ = \frac{\mathrm{d}v_{xx}}{u_{xx}} = -\frac{\mathrm{d}u_{xx}}{(1+\delta_1)v_{xx}} = \frac{\mathrm{d}v_{xy}}{u_{xy}} = -\frac{\mathrm{d}u_{xy}}{(1+\delta_1)v_{xy}} = \frac{\mathrm{d}v_{yy}}{u_{yy}} = -\frac{\mathrm{d}u_{yy}}{(1+\delta_1)v_{yy}}. \end{aligned} \tag{46}$$

The search space is then updated to $\{u^2+(1+\delta_1)v^2, vu_x-uv_x, uu_x+(1+\delta_1)vv_x, vu_y-uv_y, uu_y+(1+\delta_1)vv_y, vu_{xx}-uv_{xx}, uu_{xx}+(1+\delta_1)vv_{xx}, vu_{xy}-uv_{xy}, uu_{xy}+(1+\delta_1)vv_{xy}, vu_{yy}-uv_{yy}, uu_{yy}+(1+\delta_1)vv_{yy}, vu_t-uv_t, uu_t+(1+\delta_1)vv_t\}$. These terms transform under $\mathrm{pr}^{(2)}\mathbf{v}_2'$ as:

$$\mathrm{pr}^{(2)}\mathbf{v}_2' \begin{bmatrix} u^2+(1+\delta_1)v^2 \\ vu_x-uv_x \\ uu_x+(1+\delta_1)vv_x \\ vu_y-uv_y \\ uu_y+(1+\delta_1)vv_y \\ vu_{xx}-uv_{xx} \\ uu_{xx}+(1+\delta_1)vv_{xx} \\ vu_{xy}-uv_{xy} \\ uu_{xy}+(1+\delta_1)vv_{xy} \\ vu_{yy}-uv_{yy} \\ uu_{yy}+(1+\delta_1)vv_{yy} \\ vu_t-uv_t \\ uu_t+(1+\delta_1)vv_t \end{bmatrix} = \begin{bmatrix} 0 \\ -(vu_y-uv_y) \\ -(uu_y+(1+\delta_1)vv_y) \\ (1+\delta_2)(vu_x-uv_x) \\ (1+\delta_2)(uu_x+(1+\delta_1)vv_x) \\ -2(vu_{xy}-uv_{xy}) \\ -2[uu_{xy}+(1+\delta_1)vv_{xy}] \\ v[(1+\delta_2)u_{xx}-u_{yy}]-u[(1+\delta_2)v_{xx}-v_{yy}] \\ u[(1+\delta_2)u_{xx}-u_{yy}]+(1+\delta_1)v[(1+\delta_2)v_{xx}-v_{yy}] \\ 2(1+\delta_2)(vu_{xy}-uv_{xy}) \\ 2(1+\delta_2)[uu_{xy}+(1+\delta_1)vv_{xy}] \\ 0 \\ 0 \end{bmatrix}. \tag{47}$$

To ensure invariance under $\mathrm{pr}^{(2)}\mathbf{v}_2'$, we obtain the final perturbed differential invariants as

$$\begin{aligned} &\big\{u^2+(1+\delta_1)v^2, (1+\delta_2)(vu_{xx}-uv_{xx})+(vu_{yy}-uv_{yy}), \\ &(1+\delta_2)[uu_{xx}+(1+\delta_1)vv_{xx}]+[uu_{yy}+(1+\delta_1)vv_{yy}], vu_t-uv_t, uu_t+(1+\delta_1)vv_t\big\}. \end{aligned} \tag{48}$$

When $\delta_1 = \delta_2 = 0$, these reduce exactly to the ideal differential invariants.

Table 9: DI-SINDy results on the reaction-diffusion system under different symmetry sources. "SR" stands for success rate. All results are averaged over 50 runs. RMSE is presented as mean ± std.

Setting	SR (eq. 1) (↑)	SR (eq. 2) (↑)	SR (all) (↑)	RMSE (successful) (↓)	RMSE (all) (↓)
Ideal symmetries from visualization results of LieNLSD	**48**%	**100**%	**48**%	$(8.35 \pm 0.59) \times 10^{-3}$	$(9.53 \pm 1.26) \times 10^{-3}$
Approx. symmetries from numerical results of LieNLSD	40%	**100**%	40%	$\mathbf{(8.27 \pm 0.72) \times 10^{-3}}$	$\mathbf{(9.33 \pm 1.04) \times 10^{-3}}$
Approx. symmetries from numerical results of LieGAN	28%	0%	0%	N/A	$(1.27 \pm 0.11) \times 10^{-1}$

Table 9 presents the DI-SINDy equation discovery results under these three settings. The success rate with LieNLSD symmetries (40%) is slightly lower than with ideal symmetries (48%) but remains far superior to SINDy without symmetry, which fails completely. Notably, the RMSE metrics with

LieNLSD symmetries are comparable to (and in some cases marginally better than) those with ideal symmetries, suggesting that the numerical deviation in discovered symmetries may partially offset dataset bias. By contrast, using LieGAN symmetries (which have much larger Grassmann distance) leads to a complete failure of the joint equation system. These results confirm that the quality of symmetry discovery directly determines the quality of equation discovery, and that our pipeline can serve as a principled downstream benchmark for evaluating symmetry discovery methods. The corresponding evaluation of DI-E2E under different symmetry sources is presented in Appendix H.4.

H.4 Differential Invariants as a Plug-and-Play Module for Equation Discovery

Differential invariants provide a universal, plug-and-play mechanism for equation discovery: by reducing the search space while strictly enforcing symmetry constraints, they consistently improve any downstream method that accepts a function library or relevant terms. Here we evaluate three instantiations beyond DI-SINDy: DI-E2E (E2E (Kamienny et al., 2022) based on Differential Invariants), DI-WSINDy (Weak SINDy (Messenger & Bortz, 2021) based on Differential Invariants), and DI-PySR (PySR (Cranmer, 2023) based on Differential Invariants).

E2E vs. DI-E2E. Similar to DI-SINDy, we incorporate differential invariants as relevant terms into the pre-trained E2E model. Both E2E and DI-E2E infer an explicit expression F from a set of input data points. Note that F is represented in the form of an expression tree without a fixed skeleton, so the relevant metrics of the SINDy-based methods, such as success rate and RMSE of the coefficient matrix, are not applicable. We adopt the R^2**-score** and **accuracy to tolerance** τ from the original paper (Kamienny et al., 2022) to evaluate E2E and DI-E2E, which are defined as follows:

$$R^2 = 1 - \frac{\sum_{i=1}^{N_{\text{test}}} \|y_i - F(x_i)\|^2}{\sum_{i=1}^{N_{\text{test}}} \|y_i - \bar{y}\|^2}, \quad \text{Acc}_\tau = \frac{1}{N_{\text{test}}} \sum_{i=1}^{N_{\text{test}}} \mathbb{1}\left(\frac{\|F(x_i) - y_i\|}{\|y_i\|} \leq \tau\right), \tag{49}$$

where $\mathbb{1}$ is the indicator function, and $\mathcal{D}_{\text{test}} = \{(x_i, y_i)\}_{i=1}^{N_{\text{test}}}$ is the test dataset.

Table 10: R^2-score, accuracy to tolerance τ, and inference time of E2E and DI-E2E for the KdV, KS, Burgers, nKdV, and reaction-diffusion (RD) equations. All experimental results are averaged over 50 runs and presented in the format of mean $\pm$ std.

Name	Method	R^2 (↑)	$\text{Acc}_{0.1}$(↑)	$\text{Acc}_{0.01}$(↑)	$\text{Acc}_{0.001}$(↑)	Inference time (s) (↓)
KdV	E2E	$(5.07 \pm 3.12) \times 10^{-1}$	$(7.01 \pm 6.43) \times 10^{-2}$	$(6.57 \pm 5.40) \times 10^{-3}$	$(6.35 \pm 5.37) \times 10^{-4}$	120 ± 4
	DI-E2E (Ours)	$\mathbf{(5.51 \pm 3.19) \times 10^{-1}}$	$\mathbf{(1.04 \pm 0.81) \times 10^{-1}}$	$\mathbf{(1.13 \pm 1.38) \times 10^{-2}}$	$\mathbf{(1.08 \pm 1.17) \times 10^{-3}}$	$\mathbf{115 \pm 5}$
KS	E2E	$(7.37 \pm 12.85) \times 10^{-2}$	$(2.15 \pm 1.79) \times 10^{-2}$	$(2.19 \pm 1.86) \times 10^{-3}$	$(2.29 \pm 2.87) \times 10^{-4}$	131 ± 6
	DI-E2E (Ours)	$\mathbf{(4.40 \pm 2.38) \times 10^{-1}}$	$\mathbf{(8.80 \pm 2.90) \times 10^{-2}}$	$\mathbf{(9.02 \pm 3.66) \times 10^{-3}}$	$\mathbf{(8.47 \pm 4.02) \times 10^{-4}}$	$\mathbf{95.7 \pm 1.1}$
Burgers	E2E	$(9.94 \pm 0.10) \times 10^{-1}$	$(7.95 \pm 1.48) \times 10^{-1}$	$(1.25 \pm 0.76) \times 10^{-1}$	$(1.26 \pm 1.06) \times 10^{-2}$	109 ± 3
	DI-E2E (Ours)	$\mathbf{(9.97 \pm 0.03) \times 10^{-1}}$	$\mathbf{(8.65 \pm 0.68) \times 10^{-1}}$	$\mathbf{(2.92 \pm 1.62) \times 10^{-1}}$	$\mathbf{(3.25 \pm 4.47) \times 10^{-2}}$	$\mathbf{102 \pm 1}$
nKdV	E2E	$(2.09 \pm 2.52) \times 10^{-1}$	$(3.47 \pm 2.34) \times 10^{-2}$	$(3.50 \pm 2.54) \times 10^{-3}$	$(3.17 \pm 3.13) \times 10^{-4}$	121 ± 3
	DI-E2E (Ours)	$\mathbf{(2.77 \pm 3.17) \times 10^{-1}}$	$\mathbf{(7.72 \pm 7.08) \times 10^{-2}}$	$\mathbf{(7.03 \pm 5.56) \times 10^{-3}}$	$\mathbf{(7.57 \pm 6.67) \times 10^{-4}}$	$\mathbf{103 \pm 2}$
RD	E2E	NaN	NaN	NaN	NaN	35.0 ± 0.9
	DI-E2E (Ours)	$\mathbf{(9.99 \pm 0.00) \times 10^{-1}}$	$\mathbf{(9.62 \pm 0.13) \times 10^{-1}}$	$\mathbf{(7.04 \pm 2.51) \times 10^{-1}}$	$\mathbf{(1.94 \pm 3.71) \times 10^{-2}}$	$\mathbf{20.2 \pm 1.0}$

In Table 10, we present the quantitative evaluation results of E2E and DI-E2E for the KdV, KS, Burgers, nKdV, and reaction-diffusion equations, along with the corresponding inference times. The settings for all datasets remain consistent with those in Appendix F. Specifically, for the reaction-diffusion system, due to its vast search space, we sample only $8,192$ data points to ensure efficient inference. Although E2E generates more flexible expressions compared to SINDy, its overall performance is unstable due to noise in the dataset and errors introduced by central differencing. However, our DI-E2E demonstrates significant improvements across all metrics while requiring less computational time. Notably, E2E completely fails for the high-dimensional and complex reaction-diffusion system, whereas our DI-E2E achieves an R^2-score close to 1, which is nearly perfect.

We further evaluate DI-E2E on the reaction-diffusion system under the same three symmetry source settings used for DI-SINDy in Appendix H.3: ideal symmetries from visualization results of LieNLSD, approximate symmetries from numerical results of LieNLSD, and approximate symmetries from numerical results of LieGAN. Table 11 shows that the R^2 and Acc_τ metrics under LieNLSD symmetries match those under ideal symmetries, while LieGAN symmetries cause a significant degradation.

Table 11: DI-E2E results on the reaction-diffusion system under different symmetry sources. All results are averaged over 50 runs and presented as mean ± std.

Setting	R^2 (↑)	$\text{Acc}_{0.1}$ (↑)	$\text{Acc}_{0.01}$ (↑)	$\text{Acc}_{0.001}$ (↑)
Ideal symmetries from visualization results of LieNLSD	$\mathbf{(9.99 \pm 0.00) \times 10^{-1}}$	$(9.62 \pm 0.13) \times 10^{-1}$	$(7.04 \pm 2.51) \times 10^{-1}$	$\mathbf{(1.94 \pm 3.71) \times 10^{-2}}$
Approx. symmetries from numerical results of LieNLSD	$\mathbf{(9.99 \pm 0.00) \times 10^{-1}}$	$\mathbf{(9.63 \pm 0.11) \times 10^{-1}}$	$\mathbf{(7.17 \pm 2.17) \times 10^{-1}}$	$(1.19 \pm 1.45) \times 10^{-2}$
Approx. symmetries from numerical results of LieGAN	$(9.72 \pm 0.08) \times 10^{-1}$	$(1.68 \pm 0.32) \times 10^{-1}$	$(1.37 \pm 0.73) \times 10^{-3}$	$(4.88 \pm 23.92) \times 10^{-6}$

This mirrors the DI-SINDy finding and further corroborates that differential invariant-based methods are robust to small symmetry perturbations ($O(\delta)$ as derived in Appendix H.3), but sensitive to large symmetry errors.

WSINDy vs. DI-WSINDy. Weak SINDy (Messenger & Bortz, 2021) replaces pointwise derivative approximations with linear transformations and variance reduction techniques to improve robustness against noise. Table 12 shows that DI-WSINDy consistently outperforms WSINDy across all four equations. Notably, WSINDy fails completely on Burgers equation (0% success rate) and achieves only 2% on KS equation, whereas DI-WSINDy reaches 56% and 74% respectively. These gains mirror those observed for DI-SINDy, confirming that the benefit of differential invariant-based search-space reduction is independent of the downstream regression algorithm.

Table 12: Comparison of WSINDy and DI-WSINDy on the KdV, KS, Burgers, and nKdV equations. All results are averaged over 50 runs. RMSE is presented as mean ± std.

Name	Method	Success rate (↑)	RMSE (successful) (↓)	RMSE (all) (↓)
KdV	WSINDy	10%	$(1.30 \pm 0.57) \times 10^{-1}$	$(8.77 \pm 3.52) \times 10^{-1}$
	DI-WSINDy (Ours)	**54%**	$\mathbf{(4.92 \pm 3.45) \times 10^{-2}}$	$\mathbf{(3.52 \pm 3.29) \times 10^{-1}}$
KS	WSINDy	2%	$(2.15 \pm 0.00) \times 10^{-1}$	2.68 ± 1.54
	DI-WSINDy (Ours)	**74%**	$\mathbf{(6.25 \pm 6.30) \times 10^{-2}}$	$\mathbf{(2.35 \pm 3.09) \times 10^{-1}}$
Burgers	WSINDy	0%	N/A	$(6.83 \pm 0.67) \times 10^{-1}$
	DI-WSINDy (Ours)	**56%**	$\mathbf{(5.34 \pm 5.97) \times 10^{-4}}$	$\mathbf{(3.32 \pm 3.24) \times 10^{-3}}$
nKdV	WSINDy	30%	$(1.83 \pm 1.02) \times 10^{-1}$	$(7.55 \pm 3.79) \times 10^{-1}$
	DI-WSINDy (Ours)	**70%**	$\mathbf{(5.95 \pm 5.38) \times 10^{-2}}$	$\mathbf{(2.54 \pm 3.00) \times 10^{-1}}$

PySR vs. DI-PySR. PySR (Cranmer, 2023) uses a multi-population evolutionary algorithm and an evolve-simplify-optimize loop for symbolic regression, generating more flexible expression trees than SINDy. Table 13 shows that DI-PySR consistently improves upon PySR across all equations and metrics. The improvement is most pronounced on KS equation (R^2: $0.405 \rightarrow 0.940$) and Burgers equation (R^2: $0.634 \rightarrow 0.997$), where the original PySR struggles with large search spaces. This further demonstrates that reducing the search space via differential invariants yields substantial benefits regardless of the type of downstream equation discovery method.

Table 13: Comparison of PySR and DI-PySR on the KdV, KS, Burgers, and nKdV equations. All results are averaged over 50 runs and presented as mean ± std.

Name	Method	R^2 (↑)	$\text{Acc}_{0.1}$ (↑)	$\text{Acc}_{0.01}$ (↑)	$\text{Acc}_{0.001}$ (↑)
KdV	PySR	$(6.93 \pm 3.15) \times 10^{-1}$	$(1.51 \pm 2.19) \times 10^{-1}$	$(2.41 \pm 7.24) \times 10^{-2}$	$(3.54 \pm 14.87) \times 10^{-3}$
	DI-PySR (Ours)	$\mathbf{(8.95 \pm 2.00) \times 10^{-1}}$	$\mathbf{(5.94 \pm 3.18) \times 10^{-1}}$	$\mathbf{(1.79 \pm 1.59) \times 10^{-1}}$	$\mathbf{(4.31 \pm 7.27) \times 10^{-2}}$
KS	PySR	$(4.05 \pm 1.73) \times 10^{-1}$	$(4.29 \pm 1.55) \times 10^{-2}$	$(4.09 \pm 1.64) \times 10^{-3}$	$(4.08 \pm 3.07) \times 10^{-4}$
	DI-PySR (Ours)	$\mathbf{(9.40 \pm 0.68) \times 10^{-1}}$	$\mathbf{(3.81 \pm 1.20) \times 10^{-1}}$	$\mathbf{(5.06 \pm 2.10) \times 10^{-2}}$	$\mathbf{(5.12 \pm 2.24) \times 10^{-3}}$
Burgers	PySR	$(6.34 \pm 3.38) \times 10^{-1}$	$(3.75 \pm 3.51) \times 10^{-1}$	$(7.80 \pm 17.08) \times 10^{-2}$	$(2.31 \pm 6.61) \times 10^{-2}$
	DI-PySR (Ours)	$\mathbf{(9.97 \pm 0.04) \times 10^{-1}}$	$\mathbf{(9.39 \pm 0.34) \times 10^{-1}}$	$\mathbf{(5.16 \pm 1.29) \times 10^{-1}}$	$\mathbf{(2.50 \pm 1.30) \times 10^{-1}}$
nKdV	PySR	$(6.40 \pm 2.51) \times 10^{-1}$	$(1.17 \pm 1.55) \times 10^{-1}$	$(1.30 \pm 1.90) \times 10^{-2}$	$(1.18 \pm 1.66) \times 10^{-3}$
	DI-PySR (Ours)	$\mathbf{(7.08 \pm 3.75) \times 10^{-1}}$	$\mathbf{(4.21 \pm 3.26) \times 10^{-1}}$	$\mathbf{(1.27 \pm 1.85) \times 10^{-1}}$	$\mathbf{(4.06 \pm 9.65) \times 10^{-2}}$

I Discussion and Limitation

I.1 Dependence on Symmetry Prior

Our method requires symmetry information (infinitesimal generators) as input. We categorize application scenarios into three classes based on the availability of symmetry:

1. **Known symmetries.** Most classical scientific and engineering domains fall into this class—examples include space-group symmetries in molecular crystal structures and translational/rotational symmetries in robotic dynamics. For such systems, applying our pipeline is directly justified.
2. **Unknown but discoverable symmetries.** For more complex systems, symmetry discovery methods (Yang et al., 2024a; Ko et al., 2024; Shaw et al., 2024; Hu et al., 2025a) can automatically discover the infinitesimal generators from data. Our pipeline, combined with these methods, holds significant potential for enabling new scientific discoveries (see Appendix H.3 for details).
3. **Unknown and undiscoverable symmetries.** Our approach is not directly applicable when current symmetry discovery methods fail. However, as these methods become more powerful, an increasing number of systems will transition into class 2.

We further distinguish three types of imperfect symmetry information and analyze their impact:

1. **Incomplete symmetry.** Omitting some infinitesimal generators results in an incomplete compression of the search space but still provides correct candidates. Therefore, compared to using no symmetry at all, incorporating incomplete symmetry still yields benefits without compromising correctness. As described in Section 4.2 and Table 1, the more complete the provided symmetry, the greater the search-space reduction.
2. **Approximate symmetry.** We define approximate symmetry as symmetry that is formally correct but numerically deviant (e.g., $-1.1y\partial_x + x\partial_y$ is an approximate generator of the $\mathrm{SO}(2)$ group). As demonstrated in Appendix H.2 and Appendix H.3, our method exhibits strong robustness to approximate symmetry, and small perturbations in the generators lead to only slightly biased differential invariants.
3. **Misspecified symmetry.** We define misspecified symmetry as formally incorrect symmetry (e.g., $-y\partial_x + x\partial_y + \partial_x$ is a misspecified generator of the $\mathrm{SO}(2)$ group). Such symmetry information leads to incorrect forms of differential invariants, which can cause our method to fail completely. However, under the joint verification of automatic symmetry detection methods and domain expertise of human scientists, obviously unreasonable symmetries can be easily filtered out.

I.2 Selection of Prolongation Order

When the manually specified prolongation order n is less than the actual order of the PDE, our method fails due to the loss of crucial higher-order differential invariants. Therefore, in practice, we conservatively choose a larger n to ensure all ground-truth terms are included.

Although this may introduce additional higher-order differential invariants into the search space, it does not affect the correctness of the final equation discovery result. For example, in the main experiments—the KdV, Burgers, and nKdV equations whose actual orders are 2 or 3—we set the prolongation order to $n = 4$.

When prior knowledge of the PDE order is unavailable, we propose several principled approaches for future work:

1. **Model selection criteria.** Run the equation discovery process on candidate orders n and select the n that optimizes a criterion such as AIC or BIC.
2. **Fourier analysis.** Apply a Fourier transform to the spatial variables in the data, compute the energy spectrum, and analyze its high-frequency decay rate to estimate the highest order of effective derivatives.

3. **Symmetry discovery output.** The order of the PDE can be inferred from the highest order appearing in the infinitesimal generators output by the symmetry discovery method.

I.3 System Discoverability and the Role of Symmetry

The uniqueness of discovering dynamical systems from data is not always guaranteed. Shumaylov et al. (2025) theoretically proved that chaos is a necessary condition for ensuring the discoverability of a system in the space of continuous or analytic functions; non-chaotic systems (such as those with first integrals) often cannot be uniquely identified from finite trajectories. This result further highlights the importance of incorporating prior knowledge, such as symmetry, into equation discovery. Our method constrains the search space to physically consistent forms through symmetry-induced differential invariants, thereby restoring uniqueness even in non-chaotic scenarios. This aligns with the philosophy advocated in Shumaylov et al. (2025) of integrating physical priors to address ill-posedness.

I.4 Computational Cost

The preprocessing cost of our pipeline consists of two components: (1) symmetry discovery and (2) computation of differential invariants.

For the reaction-diffusion system, symmetry discovery via LieNLSD (Hu et al., 2025a) takes only 3–4 seconds. The derivation of differential invariants can either be done manually by human scientists (minutes to hours depending on complexity) or delegated to modern reasoning language models. Empirically, Gemini 2.0 Flash Lite takes 5–10 seconds and Claude Opus 4.6 takes 20–30 seconds for deriving the differential invariants of the reaction-diffusion system.

On the inference side, the reduction in search space achieved by our method offsets the preprocessing cost for most downstream regression models. As shown in Table 10, DI-E2E saves approximately 15 seconds of inference time compared to E2E on the reaction-diffusion system; this gap is expected to widen as the data size increases. Furthermore, once derived, the differential invariants of commonly used symmetry groups can be reused across experiments without re-computation.

When using lightweight language models (e.g., Gemini 2.0 Flash Lite), the total preprocessing overhead—symmetry discovery (3–4 s) plus differential invariant computation (5–10 s)—is smaller than the inference time saved ($\approx$15 s), making our pipeline suitable for scenarios with high response-time requirements. When using more capable but slower models or manual derivation, the preprocessing cost may outweigh the gains from search-space reduction; in such cases, our pipeline is better suited for scenarios prioritizing accuracy.